1996

Simultaneous measurement of ion ratios by inductively coupled plasma - mass spectrometry with a twin quadrupole instrument

Arnold Rockwell Warren
Iowa State University

Simultaneous measurement of ion ratios by inductively coupled plasma - mass spectrometry with a twin quadrupole instrument

by

Arnold Rockwell Warren

A Thesis Submitted to the

Graduate Faculty in Partial Fulfillment of the

Requirements for the Degree of

DOCTOR OF PHILOSOPHY

Department: Chemistry
Major: Analytical Chemistry

Approved:

Signature was redacted for privacy.

In Charge of Major Work

Signature was redacted for privacy.

For the Major Department

Signature was redacted for privacy.

For the Graduate College

Iowa State University
Ames, Iowa

1996

DEDICATION

I would like to dedicate this dissertation to my wonderful grandfather, John David Warren; although he has been gone for many years, his lessons and his love will remain with me always.

TABLE OF CONTENTS

GENERAL INTRODUCTION

The application of ICP-MS to the determination of isotope ratios was demonstrated early in the history of the technique by Houk et al (1). ICP-MS is already being used for isotope ratio measurements in nutrition, medicine, geochemistry, environmental studies, and the nuclear industry.

Isotopes are atoms which have the same atomic number (and therefore similar chemical properties), but differing mass numbers. The relative abundances of two different isotopes can be either *natural*, which is to say the result of the amounts formed early in the history of the universe and/or the products of natural radioactive decay, or *artificial*, where the natural ratio has been altered, as in the incorporation of man-made nuclides from an atomic reactor or as the result of the detonation of a nuclear device. The variations in isotope ratios are very useful as indicators of the geological age or area of origin of a material, as well as its history, in the case of artificially produced radionuclides residing in nuclear waste storage facilities. Stable nuclides are used in nutritional uptake research, while in the field of environmental studies, certain tracer isotopes are used to follow the distribution patterns of substances released into the environment. The change in isotope ratio which needs to be determined in these cases can be <1%, requiring precisions

of <0.3% RSD to differentiate between samples.

Isotope ratio measurements are also used for determining elemental concentrations in a sample by the technique known as *isotope dilution*. This method is capable of highly accurate and precise determinations of an element which has two or more stable isotopes. The natural ratio between two isotopes in the sample is altered by the addition of an accurately known quantity of an isotopic spike. Measurement of the resultant ratio of the mixture allows the calculation of the original concentration of analyte present, providing that the weight of the sample, the weight of the spike, and the various ratios of sample, spike, and mixture are known.

There are several methods of determining the isotope ratio of an elemental species using mass spectrometry: thermal ionization mass spectrometry (TIMS), secondary ion mass spectrometry (SIMS), electron impact (EI), and inductively coupled plasma mass spectrometry (ICP-MS). For metals, TIMS has been the most widely used, chiefly due to its high precision (commonly 0.1 - 0.01 % relative standard deviation (RSD)). However this technique has several drawbacks. In TIMS, sample aliquots are deposited on a rhenium or tungsten filament which is then placed in the source of the mass spectrometer and heated to generate atomic ions for elemental analysis. Usually the analyte must be separated from the matrix and then mounted uniformly on the

filament, a process which invariably involves considerable sample pre-treatment and chemical separation. These sample preparation steps are time-consuming and increase the risk of contamination. The time required for analysis is also relatively long, often taking several hours per sample; on a turret-style device, a series of samples and standards can take a day after being placed in the machine. Consequently, sample throughput rates are low, even with multiple-filament 'turret'-style devices in the source. Another drawback to TIMS is that it is limited to elements with relatively low ionization energies, unless operated in the negative ion mode. Finally, the instruments themselves require a considerable monetary investment, both in initial purchase price and maintenance. It is, however, against this standard that isotope ratio measurements by ICP-MS must be measured.

ICP-MS has a number of advantages for isotope ratio measurement. Nearly all of the metallic elements and most non-metals can be determined without switching the instrument over to a negative ion detection mode (which must be used in TIMS for elements with high-ionization potentials, such as osmium). Sample preparation is minimal, unless there are isobaric overlaps which require separation of the analyte from the matrix. Several elements can be determined at the same time, and the average analysis takes minutes instead of hours. A typical quadrupole-based ICP-MS machine is also less

costly to purchase and maintain than a TIMS instrument with its sector mass spectrometer. The chief disadvantage is that, for elements which can be analyzed by either TIMS or ICP-MS, the precision and sensitivity are poorer for conventional quadrupole ICP-MS, where precision is routinely 0.3% RSD.

In recent years, a new type of ICP-MS instrument, one which employs a sector mass spectrometer and multiple faraday cup detectors, has been developed and is now rivaling the TIMS instrument in performance. The double focusing instrument, however, is very large and expensive (~$800,000) at present. A quadrupole ICP-MS device which measures isotope ratios truly simultaneously might lead to improved precision in a smaller, less complex, and less costly device. This research presents the results from a unique double beam ICP-MS device which uses two separate quadrupole mass filters and detectors. The main thrust of this research has been the development of a quadrupole-based ICP-MS machine with improved precision for isotope ratio measurement. Several workers have shown that true simultaneous measurement of signal ratios in ICP atomic emission spectrometry (AES), rather than sequential measurements, can yield improved precision (2,3). These researchers showed that flicker noise in the plasma cancels in the resulting ratio of line intensities. This observation, and the success of the ICP-multicollector MS, led to the idea of using simultaneous signal measurement in quadrupole ICP-MS.

In all quadrupole-based ICP-MS instruments to date, the measurement of ions, whether in a scanning mode or a peak-hopping mode, is done sequentially in time, with some value of dead time for each channel being measured. Although the device can hop between peaks very rapidly (i.e., with a dead time of ~3ms) (4), it is still not truly simultaneous.

Following the double beam in space concept used in spectrophotometers, a device was constructed to divide the ion beam from an ICP into two beams, each of which is directed into a separate quadrupole mass filter with its own detector. Thus, each quadrupole statically monitors a single isotope, the thought being that any fluctuation of analyte ions in the ICP would affect the signal in both channels simultaneously, with little effect on the ratio. To the best of our knowledge, this concept of a double-beam, twin-quadrupole device has not been reported previously with the ICP or any other ion source.

DISSERTATION ORGANIZATION

This dissertation describes the performance of the twin-quadrupole ICP-MS device in the areas of applied analysis and as a diagnostic tool for investigations of ion production processes occuring within the ICP itself. This dissertation is presented such that each chapter is a paper that stands

independent of the others as a complete scientific manuscript including tables, figures, and literature cited. Additional literature citations from the general introduction and summary are given after the summary.

The first paper describes the principles and design of the new instrument, while the second paper describes the initial performance of the device. The third paper examines the effect of a matrix interferent on signals from different isotopes of the same element or elements. The fourth paper examines the effect of aerosol gas flow rate on ionic species and the correlation of the signal ratios of those species.

1. DESIGN AND DEVELOPMENT OF A TWIN QUADRUPOLE ICP-MS INSTRUMENT

A paper submitted to Applied Spectroscopy

A. R. Warren and R. S. Houk

BACKGROUND

The idea for this project came from an idea proposed by Morteza Janghorbhani (1-2). One of Janghorbhani's areas of research deals with the uptake of minerals which are nutritionally important to the human body. Such research often requires precise measurement of isotope ratios in stable isotope tracer experiments. In a tracer experiment, the test subject is given a special diet which has been enriched in a stable isotope of the element of interest. After sufficient time has passed, the isotope ratio of that element is measured, and the deviation of the measured ratio from the natural ratio is used to calculate the percentage of the element which has been absorbed by the body. Only a small amount of the stable isotope can be reasonably introduced, so

the change in the natural ratio is often quite small, hence the need for precise measurements.

Conventional quadrupole ICP-MS instruments are used for trace element research due to their low detection limits; however, the routine precision of ratios obtained from such instruments is not adequate for many of the elements of interest. Janghorbhani suggested that the *simultaneous* measurement of ratios would improve their precision, and there are good reasons why this would be so. A common method of measuring ratios with a quadrupole involves the method of *peak hopping*, whereby the quadrupole allows first one, then the other isotope to be counted at the detector, with a certain amount of time in between each measurement necessary for the resetting of instrumental voltages and the stabilization of electronic components. A crucial component of the precision of such sequential measurements is the stability of the source. Unfortunately, it has been observed that the plasma itself has several noise components (3-7) and that it also flickers on a short time scale (8). Use of short scans across the two isotopes is another technique for ratio measurement, but this still involves a time differential between the counting of each isotope. Houk reasoned that by splitting the beam of ions into two beams, and introducing each beam into its own quadrupole and detector would allow the simultaneous measurement of the ratio.

To measure two ions simultaneously, it was obvious that the design required two mass filters and detectors, and a means of dividing the extracted beam of ions into two beams representative of the initial beam. An atmospheric extraction interface attached to a vacuum chamber containing the lenses and mass filters was needed, and an inductively coupled plasma torch was modified to operate as an ion source for the instrument.

THE BEAM SPLITTER

Before construction of a vacuum chamber for this new instrument, the method of splitting the ion beam had to be decided, as this would delineate the geometrical constraints for the chamber design. Two methods of splitting the beam presented themselves, one using magnetic fields, as is done in particle accelerators, and the other using electrostatic fields. The low energies (3-10 eV) of the beam extracted from an ICP would make magnetic separation, which is most effective with high-energy (keV-GeV) beams, difficult. Using magnetic separation would involve acceleration of the particles, and then, to meet the energy criteria for the quadrupoles, deceleration. Such a process would complicate the instrument and introduce more sources of noise into the measurements. On the other hand, an electrostatic field is more amenable to

the deflection of low energy beams, and would involve little additional electronics; only controlled potential sources would be needed to create the necessary fields. Therefore, it was decided that an electrostatic element would best fit the requirements for a beam splitting device.

Electrostatic fields are best known for their application as energy selectors in many types of analytical devices. In principle, an electrical field is formed between two plates which are held in relatively close proximity to each other (the distance between the plates is typically governed by the energies of the particles to be analyzed as well as the spread of energies involved), and field lines of equal potential (E_o) are formed between the charged plates. A particle entering the gap between the plates with an energy equal to that of a particular field line ($E=E_o$) follows a path delineated by that particular field line. The literature contains many examples of electrostatic sectors, but as far as the author of this paper knows, none of the applications involve splitting of a low energy beam of particles. Most applications involve either energy filtering of particles within the beam (as in the hemispherical analyzers used in photoelectron spectroscopy or quadrupole mass filters) or simple redirecting and shaping of the beam (as in electrostatic hexapoles and deflectors). The author believes that this is the first design of an electrostatic element

which is used to divide a beam of low energy atomic ions and direct the resultant beams in two different directions.

The idea behind the beam splitter came from drawing an analogy between a beam of ions and a stream of water. Water follows a path of least resistance according to gravity and the conditions of the terrain. Similarly, charged particles follow field lines and gradients. In order to study the behavior of different geometries in electrostatic elements, a computer program, SIMION, was used extensively. SIMION was developed by D.A. Dahl and J.E. Delmore at Idaho National Engineering Laboratory under contract by the Department of Energy. This program allows the experimenter to input the geometry and potential of an electrostatic element, to observe the field gradients which are formed, and then to simulate the trajectories of charged particles through those gradients. The experimenter can alter the shapes of charged elements and their potential, and can change the mass and velocity (i.e. the energy) of the particles traversing the fields which are formed.

The initial designs all incorporated a central, sharp-edged element which physically intercepted the beam along its axis. Of course, this design would completely stop ions which were exactly on axis, but here is where one of the problematic qualities of a low energy ion beam, space-charge repulsion, worked to our advantage. This space charge causes the beam to

expand in cross section as the entrained positive ions experience a mutual repulsion from each other. In our case it was hoped that the expansion caused by space charge would result in more ions following paths slightly outside the central axis. Such particles would not strike the front edge of the splitter, but would instead enter the spaces between the central element and the outside elements and be directed along the desired path along field lines created between the charged elements. Initial designs involved angled flat plates, but simulations showed that the particles followed divergent paths upon exiting the splitting device. This problem was tested during development by using a bent grid to split and deflect the beam 90°, an experiment which yielded too few ions to be acceptable. Research on curved electrostatic sector designs yielded a solution in the form of toroidal electrostatic sectors. The toroidal shape was chosen as a compromise between a spherical shape, with better focusing and beam convergence, and planar elements which would present the least blockage to the ion beam at the entrance.

The next decision which had to be made was the angle at which the ion beams would be deflected into the quadrupole entrance plates. The mathematical treatment of curved sectors yields several 'special' angles for electrostatic elements which impart different characteristic profiles to the exit

beam. An angle of 30° was chosen in this case, as it was very close to the "magic" angle of 31° 50', an angle which yields a nearly collinear exit beam of ions.

The final consideration was the spacing between the charged surfaces of the splitter. In this we were somewhat constrained by the fact that the quadrupole entrance plates could only be brought so close together without physically touching each other. Also, the RF fields of the quadrupoles could interfere with each other. The author also had the idea that a wider gap between the sector plates would entrain more of the expanded ion beam.

The final design for the beam splitter is shown in Fig 1. It consists of two toroidal sectors placed back to back. The sectors share the central element. The beam splitter was constructed from stainless steel for rigidity and its elements were cut from solid blocks to accommodate the difficulty of machining the complex surface curves. The inner surfaces were hand-finished and polished to a mirror-like finish, which is necessary for producing homogenous electric fields. After the three sections were fabricated, they were mounted on a lexan block and isolated from it with nylon washers.

THE VACUUM CHAMBER

The vacuum chamber for the twin quadrupole instrument is shown in Fig. 2. The vacuum chamber itself is made of steel and incorporates two of the three differential pumping stages. The first stage was created by a stainless steel spacer ring mounted to the skimmer flange which was pumped by a large mechanical pump to approximately one torr. The second stage was kept at 10^{-3} torr by a large diffusion pump, and the third stage was held at 10^{-6} torr by two small turbomolecular pumps, which were later replaced with one large turbomolecular pump. The chamber dimensions were specified using the mechanical drawings of the Extrel quadrupole mass spectrometers which we planned to acquire. Later in the construction of the instrument, superior quadrupole systems from Fisons Instruments (VG) were acquired, and this system was acquired. Unfortunately, the VG quadrupoles were shorter in length than the Extrel units, and the vacuum chamber had already been constructed at no small cost. This resulted in the distances from the exits of the beam splitter to the quadrupole entrances to be almost 10 cm longer than planned, and sets of cylindrical lens elements were placed in the gaps to compensate. The quadrupoles themselves were controlled through a voltage input to the RF controllers to set the mass. These control voltages were input from a personal computer

using an Intel 386 chip running at 33MHz. This computer also performed all of the data collection and provided statistical calculations through the use of Asyst, a scientific programming language which is well-suited to controlling instruments and collecting data in real time. The detectors which were used in the quadrupoles were of the continuous-dynode "channeltron" type, and in the initial stages, each detector had its own high-voltage power supply. The pulses from these detectors were discriminated and counted using specialized electronic components from EG&G. The dual counter/computer system collected signals from both channels of the instrument as nearly simultaneously as was possible. Ho-Ming Pang's considerable expertise in computer programming was very helpful in setting up programs to do the various tasks necessary for data acquisition.

For the plasma itself, we modified a vertically mounted torch so that it could be operated in the horizontal direction. This modification necessitated building a new shielding box to confine the RF energy and protect the eyes of the operator from the intense light. The torch box was mounted on a movable x-y-z stage which in turn was mounted on a modified lathe rail so that the entire torch assembly could be moved into place once the plasma had been ignited. With the final installation of adequate power and cooling water supplies, the instrument was ready for initial testing.

INITIAL TESTS

Our first tests, with the splitter and both quadrupoles in place, were not encouraging. So little signal was seen that there was some doubt as to whether the ion sampling process was operating as it should. To test this, the splitter was removed, and a single quadrupole was placed on the central axis of the instrument. The quadrupole entrance in this position was more than 20 cm from the third stage aperture, and fewer than 20,000 counts were seen with an analyte solution which should have yielded millions of counts. Still, the response was positive, and the instrument was returned to its original configuration. Countless hours were spent in moving the splitter to find the ion beam focus. It seemed that the beam axes exiting the splitter were not exactly parallel, and the ion counts were still quite low. Going back to the literature on electrostatic sectors, two elements were added to the beam splitting device. The first addition was a set of four beam shift plates, which were added between the differential pumping aperture and the entrance of the beam splitter. The idea behind this was to modify the cross-sectional profile of the beam to place more ions into the twinned channels on either side of the sharp central element. The effect of this element was readily observed, as the ion counts through the splitter followed a

change of the voltages on the plates. Originally it was a true electric quadrupole, but then the right and left plates were electrically separated and connected to separate potentials, which allowed us to use them as beam-shift plates as well.

The second addition was suggested by an article by Wollnik (9), and consisted of fringing-field plates placed just outside the exits of the beam splitter. Ion counts increased into the hundreds of thousands, and the first isotope ratios were measured for a solution of 100 ppm silver.

FURTHER DEVELOPMENTS

While it was possible to measure isotope ratios with the new instrument, the concentration of analyte solutions needed to supply sufficient counts was very high. Several other modifications were considered to improve the ion sampling efficiency of the interface and the conductance through the electrostatic beam splitter.

While fringing field plates had been placed at the exits of the beam splitter, the entrance of the splitter remained unmodified. In lieu of fringing field plates at the entrance of the beam splitter, a large, grounded wire grid was placed over the entrance of the beam splitter, the purpose of which was to isolate the analyte ions from the intense field

gradients induced by the sharp-edged central element, allowing more of the beam to enter the centers of the two channels with little deflection.

In addition, a change to the operating voltages of the splitter was made, due to higher-than-typical ion energies in the plasma due, it was believed, to a secondary discharge at the sampling interface. In the beginning, the operating voltages on all splitter elements were within the range of 0 to -10 volts. It was found that increasing the potentials on the splitter negatively resulted in a substantial increase in signal.

The third improvement was made accidentally while checking the detectors. Upon replacement of one of the old channeltrons with a fresh one, the sensitivity of one channel was increased by more than a factor of ten.

With the addition of the grid, the splitter voltage changes, and the replacement of the old detectors with new ones, 1 ppm analyte solutions could be measured with the same signal level that was previously obtained only with 100 ppm concentrations, a considerable improvement in sensitivity.

High background counts were a problem with the instrument, precluding the analysis of low abundance ions. The mirrored inner surfaces of the beam splitter reflected light from the plasma back to the detectors, giving a substantial background. The inner surfaces of the beam

splitter were coated with a conducting layer of graphite (Aerodaq-G, Atcheson Colloids Co., Port Huron, MI). This coating absorbed the stray photons and reduced the background count rate from 80 -100 counts s^{-1} to 10 - 20 counts s^{-1}.

LITERATURE CITED

1. M. Janghorbhani, Prog. Food Nutr. Sci. 8, 303-332 (1984).

2. B. T. G. Ting and M. Janghorbhani, Spectrochim. Acta 42B, 21-27 (1987).

3. R. K. Winge, D. E. Eckels, E. L. DeKalb and V. A. Fassel, J. Anal. At. Spectrom. 3, 849-855 (1988).

4. J. S. Crain, R. S. Houk and D. E. Eckels, Anal. Chem. 61, 606-612 (1989).

5. G. P. Russ III, *Applications of ICP-MS*, A. R. Date and A. L. Gray, Eds. (Blackie, London 1989), p. 108.

6. N. Furuta, J. Anal. At. Spectrom. 3, 868-875 (1988).

7. A. L. Gray, J. G. Williams, A. T. Ince and M. Liezer, J. Anal. At. Spectrom. 9, 1179-1181 (1994).

8. R. K. Winge, J. S. Crain and R. S. Houk, J. Anal. At. Spectrom. 6, 601-604 (1991).

9. H. Wollnik, *Optics of Charged Particles*, (Academic Press, Orlando 1987).

Fig. 1. Photo of Beam Splitter

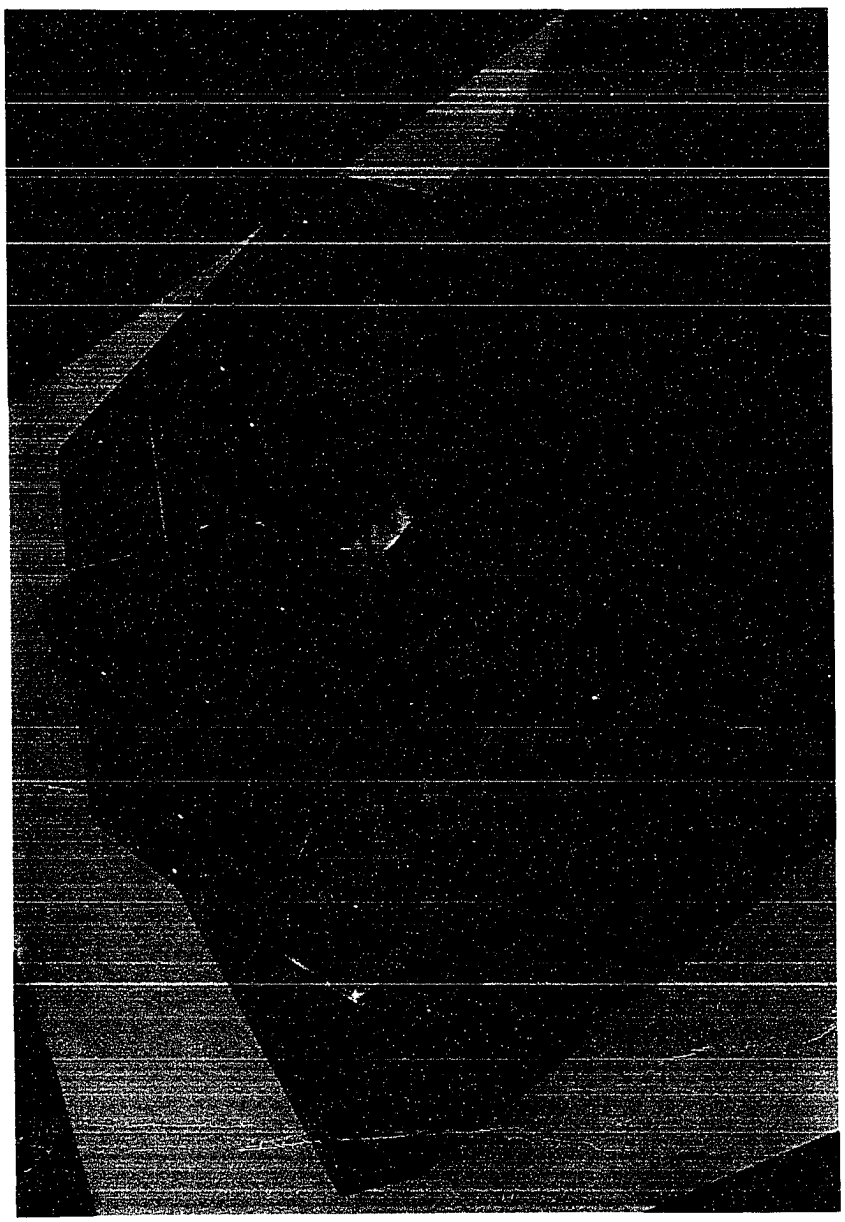

Fig. 2. Photo of Vacuum Chamber

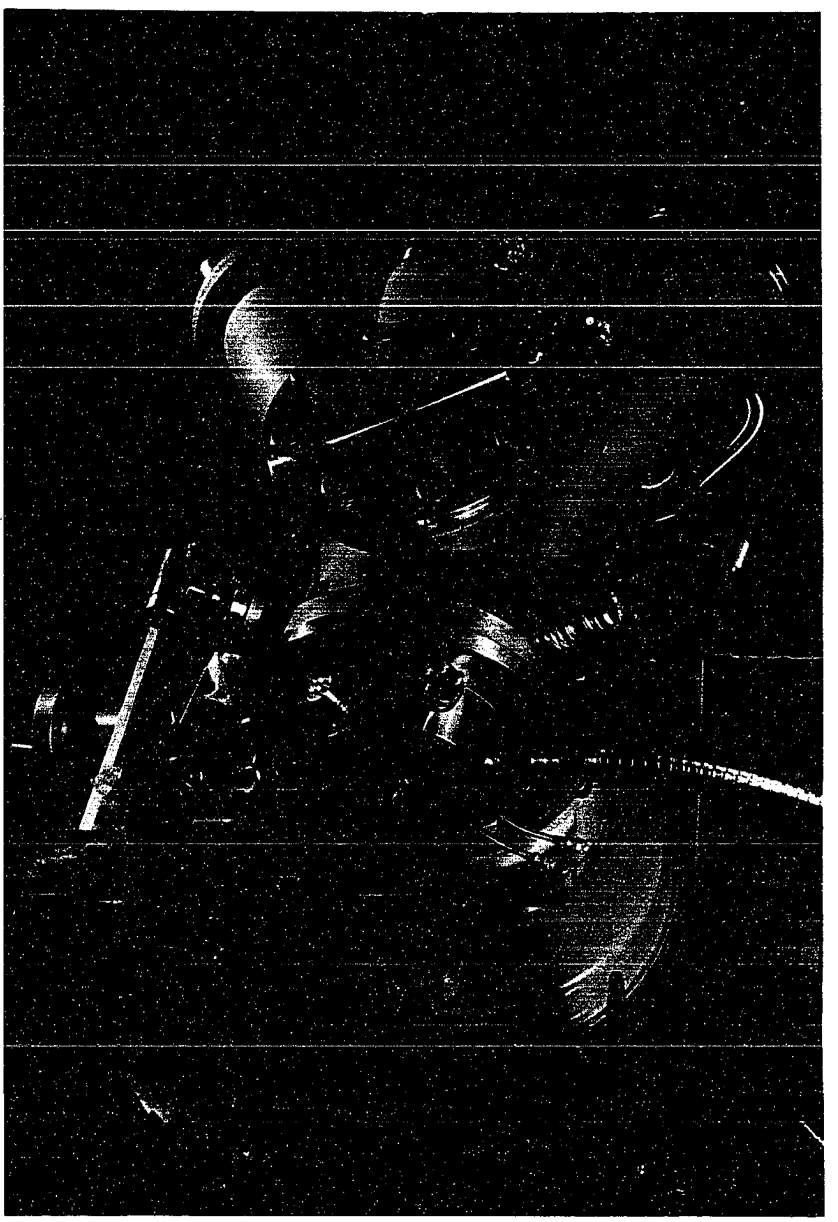

2. SIMULTANEOUS MEASUREMENT OF ION RATIOS BY INDUCTIVELY COUPLED PLASMA-MASS SPECTROMETRY WITH A TWIN QUADRUPOLE INSTRUMENT

A paper submitted to Applied Spectroscopy

A. R. Warren, L. A. Allen, H-M Pang, R. S. Houk and M. Janghorbani

INTRODUCTION

ICP-MS has developed into a very valuable method for elemental and isotopic analysis. However, the precision achievable by ICP-MS is rather limited. Single quadrupole devices can measure isotope ratios with a precision of 0.1% relative standard deviation (RSD) at best. Often, the precision is substantially poorer, particularly for very large or very small isotope ratios (1-10). For conventional elemental analysis, internal standardization is generally used to help improve precision, although the RSD of an internal standard ratio is seldom better than 1% (4). Precision is

still worse for transient samples such as those produced by flow injection analysis (FIA), electrothermal vaporization, laser ablation of solids, high performance liquid chromatography, or noisy, steady state signals that are generated by repetitive laser ablation or by arc/spark atomization of solids.

The physical reasons why precision in ICP-MS is poorer than that obtained in ICP atomic emission spectrometry (AES) are not fully understood. In this respect, ICP-AES has the advantages that the signals are spatially integrated and that the dependence of signal on aerosol gas flow rate or observation position is much more gradual than is the case in ICP-MS (11-13). Nevertheless, several workers have shown that true simultaneous measurement of signal ratios, rather than sequential measurements, can improve precision substantially in both ICP techniques. For example, Myers and Tracy (14) and Belchamber and Horlick (15) measured various emission lines simultaneously with two separate monochromators. Mermet and Ivaldi performed a similar experiment with an echelle instrument and segmented charge coupled detector (16). These three groups showed that flicker noise from the plasma cancels in the resulting ratio of line intensities. Simultaneous measurement of the background, as well as the spectral line, also eliminates flicker noise and improves signal-to-noise ratio and detection limits (17). Travis et al. use a double

beam interferometer with an ICP source. The resulting spectrum is much less susceptible to noise from intense peaks that normally gets distributed into all wavelengths with a single beam Fourier transform instrument (18).

In ICP-MS, Freedman, Walder and co-workers use a double focusing magnetic sector mass spectrometer with multiple Faraday cup collectors with an ICP ion source. In this fashion, isotope ratios are measured simultaneously without scanning. The precision of the resulting isotope ratios is ~0.01% RSD and is at least as good as that achievable by thermal ionization, the long-time champion of the highest precision in inorganic isotope ratio measurements (19-21).

Unfortunately, the sector technology necessary for measuring multiple isotope ratios simultaneously is very large and expensive (~$800,000) at present. A quadrupole ICP-MS device that measures ion ratios truly simultaneously (i.e., without scanning or peak hopping) might lead to the desired improvements in precision in a much smaller and less complex device. This paper presents initial results from a unique double beam device using two separate quadrupole mass analyzers and detectors. The ion beam from the ICP is split into two parts, and each quadrupole transmits a different m/z value. To the best of our knowledge, this concept of a double-beam quadrupole device has not been reported previously, with either an ICP or any other ion source.

EXPERIMENTAL

Twin Quadrupole Apparatus.

A diagram of the device is given in Fig. 1. The main components and operating conditions are identified in Table I. Aqueous samples are nebulized with an ultrasonic nebulizer (24) and then desolvated. In our experience, this desolvation step removes the troublesome wet droplets from the aerosol stream (25-28), although solid particles are undoubtedly still present. The resulting aerosol is injected into a horizontal argon ICP. A conventional sampler, skimmer and ion lens (29) transmit ions through the differential pumping aperture into the third vacuum stage. Here the ions pass through a set of four flat beam-shift plates and then enter the beam splitter, which is essentially two electrostatic analyzers back-to-back. The beam splitter intercepts the ion beam and deflects part of the beam through each of its two channels. After the ions leave each channel, each beam is focused into its own mass analyzer (not shown). Typical voltages used to maximize ion signals are given in Table II. These voltages vary somewhat from day to day, particularly for the beam-shift plates and beam splitter.

Each mass analyzer has a separate voltage supply and control and its own Channeltron electron multiplier operated in the pulse counting mode. Pulses from the detectors are

preamplified and discriminated and then counted using a dual counter/timer (Model 994, EG&G Ortec). The two counters open within 25 ns of each other. They stay open for a period called the dwell time, which is 2.0 s unless specified otherwise. The counters then close within 25 ns of each other, i. e., at virtually the same time. There is a 50 us delay between adjacent openings. Since the dwell time is much longer than these delays, the two counters measure the split ion beams essentially simultaneously.

Beam Splitter.

The beam splitter is shown in detail in Fig. 2. Pertinent dimensions and radii are given in Table III. Each side of the beam splitter is a toroidal condenser with a deflection angle of 30°. This angle is close to that used in the Mattauch-Herzog geometry (31.83°) and thus should yield a beam that is essentially parallel in the horizontal plane (30,31). In the vertical plane, often called the Z axis in MS parlance, the curvature of the plates should provide some weak focussing. Spherical analyzers, which should focus the beam to a point in both horizontal and vertical directions, were considered initially but were not employed because the entrance blocked too much of the beam.

The plates of the beam splitter are machined from stainless steel and coated with a conducting graphite layer (Aerodaq - G, Acheson Colloids Co., Port Huron, MI). The

graphite layer greatly reduces the background from reflected light from the plasma. The shielding grid at the entrance and the fringe field plates (32,33) play important roles. Transmission of ions is very poor and erratic without these shielding components.

Operating Conditions and Procedures.

These are identified in Table I. Generally, the plasma conditions and lens voltages were selected to provide the maximum ion signals for the desired elements. The sample concentration was generally 10 ppm in 1% HNO_3 in deionized distilled water. This concentration yielded ion count rates in the general range of 10^5 counts/s, which is near optimum for minimizing the effects of counting statistics on precision.

The transmission through the beam splitter and the bias (i.e., the transmission through one side relative to that through the other) are very sensitive to the voltages on the beam shift plates between the differential pumping orifice and the entrance grid. The relative transmission through the two sides can be altered over a wide range, or the ions can be deflected through only one side, if desired.

Analyte solutions were prepared by diluting 1000 ppm single element standards with 1% HNO_3 in deionized distilled water. The analyte concentration was generally 10 ppm. A series of isotopically altered Cu standards was prepared by

mixing weighed aliquots of enriched ^{65}Cu spikes (99.70% ^{65}Cu, Oak Ridge National Laboratory) with natural Cu in known amounts so that the total copper concentration was kept at approximately 10 ppm.

RESULTS AND DISCUSSION

Mass Spectra.

Spectra of copper ions through both mass analyzers are shown in Fig. 3. The two copper isotope peaks are clearly visible, as are small peaks from ArO^+ at m/z = 56. The peak shapes are similar to those normally seen from quadrupoles. The background is ~30 counts/sec. The sensitivity for ^{63}Cu is only ~10^4 counts/sec per ppm , which is rather low. An ultrasonic nebulizer on a quadrupole ICP-MS device would normally yield over 10^7 counts/sec per ppm. As yet, it is unclear where the ions are lost. If the voltages on the beam shift plates are adjusted to send all the ions through only one side of the beam splitter (Fig. 1), the sensitivity is poorer than the sum of the sensitivities of both quadrupoles when the beam is being split through both sides. This observation may indicate that the poor ion transmission is caused mainly by factors other than the beam splitter, although it is also possible that most of the ions simply strike the central section of the beam splitter in either

case.

Precision of Isotope Ratios.

Plots of ion count rate vs. time are given in Figs. 4 and 5 for the shortest dwell time tested (50 ms) and for the optimum dwell time (2 s). Each signal is rather noisy, with an RSD of 8.5% for the short dwell time and 4.5% when the dwell time is increased to 2 s. However, the noise in both mass analyzers seems to be correlated, at least on the time scales shown. The synchronized fluctuations in the two copper signals are very similar to those seen for emission signals by Myers and Tracy (14).

The ratio precision for $^{63}Cu^{+}/^{65}Cu^{+}$ is shown for various dwell times in Table IV. The RSD improves to 0.38% as dwell time increases; exactly the opposite trend is seen with single quadrupoles (1,2). If the dwell time is too long (e.g., 5 s), the precision deteriorates, for reasons that are unclear. Perhaps the transmission of the quadrupoles and the gain of the detectors drifts slowly in opposite directions with time. The precision at the optimum dwell time (2 s) can be improved further by averaging every 5 ratios. The RSD of 8 such averaged ratios is 0.14%. This precision is comparable to the best obtainable from single quadrupoles after 12 years of commercial development, whereas the twin quadrupole device is a mere prototype and has not yet undergone the protracted stability development program of commercial ICP-MS devices.

This value for precision is also comparable to that obtained if an array of Channeltrons is used with the ICP multicollector mass spectrometer (34). Thus, instability of the detectors may well be a limiting factor in precision, as has long been suspected.

The precision of the determined ratios is also compared to that expected from counting statistics in Table IV. The latter values are calculated as follows. Suppose n_i counts are measured during each dwell time for isotope i, and no background correction is necessary. For each signal, the standard deviation expected from counting statistics alone would be $(n_i)^{1/2}$. The RSD of the ratio R would then be $RSD_R = (1/n_{63} + 1/n_{65})^{1/2}$.

As shown in Table IV, the RSD of the measured ratio is poorer than that expected from counting statistics. Although the difference between the measured precision and the counting statistics expectation is not great, application of the F test (35) shows that the measured precision is statistically poorer in each case.

In ICP-AES, Mermet and Ivaldi have shown that signals measured from the same lines in different orders are correlated if the line intensities are high enough to minimize shot noise (16). They illustrate this correlation effect by plotting one intensity vs. the other and fitting a straight line. A correlation coefficient of between 0.95 and 1.0

indicates reasonable correlation and effective cancellation of flicker noise from each measured intensity when the ratio is calculated (16).

A typical correlation plot for Cu isotopes is shown in Fig. 6. The correlation coefficient (0.9973) is close enough to unity to indicate that the signals are indeed correlated. This correlation holds up well even though the range of fluctuations is very large, i.e., between 75 and 105 units, which is much greater than the range of 5 units (out of 100) seen in the emission studies (16). This high degree of correlation indicates that flicker noise, such as fluctuations in ion signal caused by instability of the nebulizer or plasma, cancels when the Cu isotope ratio is measured simultaneously with this twin quadrupole device.

Mass Bias Calibration.

As mentioned in the previous section, the measured isotope ratio does not equal the actual isotope ratio. The extent of this mass bias effect depends strongly on the voltages applied to the beam shift plates and the beam splitter (Fig. 1), so calibration procedures are necessary to relate the measured isotope ratio to the true one. For this purpose, a series of copper solutions were analyzed that were enriched with known amounts of ^{65}Cu.

A typical plot of (measured isotope ratio) vs. (actual isotope ratio) is given in Fig. 7. The point at the upper

right corresponds to the natural abundance sample. The measured ratio is 2.03. Therefore, the bias in this case is (true value - meas. value)/true value = (2.24 -2.03)/2.24 = 9.4%. Since the Cu isotopes are two m/z units apart, this corresponds to a bias of 4.7% per m/z unit. The extent of bias is somewhat greater than the typical values of 1% to 3% per m/z unit usually seen in this m/z range with conventional single quadrupole ICP-MS devices (2-6), as expected because of the delicacy of the ion beam splitting operation.

The other points shown in Fig. 7 correspond to the isotopically enriched samples. The measured ratio decreases with the true ratio in an approximately linear fashion. The points shown were measured in sequence from right to left as shown in the figure, and there seems to be a tendency for the measured ratio to wander below the regression line at first, then above it, and finally below it again for the point at the lower left. We attribute the slight S-shaped curvature in Fig. 7 mainly to drift. Some five minutes are required to measure each point, including the rinse out time for the nebulizer. The relative sensitivity of the two channels probably drifts during this interval. A similar S-shaped drift in the measured isotope ratio was also reported by Begley and Sharp (1), although the time period involved was much longer (several hours). Despite this modest drift, Fig. 7 shows that the measured isotope ratio can be related to the

actual isotope ratio by a calibration procedure.

Internal Standardization.

The time behavior of signals for $^{59}Co^{+}$ and $^{139}La^{+}$ is shown in Fig. 8. These signals result from the continuous nebulization of a 10 ppm standard containing both elements. Each ion signal is rather noisy, with an RSD of ~3%. However, the figure shows that the fluctuations in each signal are similar, and the ratio (Co^{+} signal)/(La^{+} signal) has an RSD of 1.2%. This RSD value for the ratio is comparable to the best precision seen in internal standard ratios with commercial single quadrupole devices (4).

A plot of Co^{+} signal vs. La^{+} signal (Fig. 9) has a correlation coefficient of 0.9332. The scatter in Fig. 9 for the internal standard ratio is much worse than that in Fig. 6 for the Cu isotope ratio and is the worst for any of the correlation plots examined in this study. Apparently, while the flicker noise in the plasma largely cancels when the ion ratio Co^{+}/La^{+} is measured simultaneously, some noise still remains. Thus, the RSD of this internal standard ratio (~1%) is not as good as that for an isotope ratio; this is commonly seen in ICP-MS. For this internal standard ratio, the measured precision is approximately ten times higher than the counting statistics limit of ~ 0.1 %.

It is also interesting to note that ions at widely different m/z values ($^{59}Co^{+}$ and $^{139}La^{+}$) can traverse the beam

splitter with just one set of applied voltages. In ICP-MS, collisions in the supersonic expansion accelerate all ions to the same velocity. Thus, ion kinetic energy increases with mass (36,37). Although $^{59}Co^{+}$ and $^{139}La^{+}$ can both traverse the beam splitter, we have experienced difficulty observing $^{59}Co^{+}$ and $^{208}Pb^{+}$ through both channels of the instrument simultaneously. It may be necessary to adjust the voltages to the outside plates of the splitter separately in such cases where the ions to be measured are at very different m/z values.

Precision for Transient Samples.

Flow injection was used to produce transient signals with a time duration of ~ 30 s, which is similar to that of a liquid chromatographic peak or a burst of particulates from a single laser shot onto a solid. The resulting FIA peaks for Cu isotopes are shown in Fig. 10. The RSD of the area of the peaks is 6-7%, while the RSD of the Cu isotope ratio is 0.91%. Again, this precision value for the ratio is comparable to the best performance seen from single quadrupole devices for transient samples. Actually, this precision value is also comparable to that expected if the same dwell time (0.3 s) had been used during continuous introduction of sample (see Table IV). The correlation plot (not shown) has a correlation coefficient of 0.9960.

On this particular day, the isotope ratio for Cu is 1.97,

i.e., a bit different from the value of 2.03 cited above. Apparently, the mass bias is sensitive to small day-to-day adjustments of the voltages on the splitter and shift plates. Such day-to-day shifts in mass bias are common in quadrupole ICP-MS devices.

Results from a similar FIA experiment for internal standardization with Co^+ and La^+ are depicted in Fig. 11. The RSD of the peak areas is 18%, while the RSD of the Co^+/La^+ signal ratio improves to 3.0%. The correlation plot (not shown) has a correlation coefficient of 0.9872, which is still close enough to unity to indicate a high degree of correlation between the Co^+ and La^+ signals, even though they fluctuated over a very wide range (60 to 100 units).

CONCLUSIONS

These results demonstrate the basic feasibility of improving precision by using two quadrupoles to measure two different m/z values simultaneously. The high degree of correlation between the two signals indicates that flicker noise is eliminated for isotope ratios and diminished for internal standard ratios. Ratio precision is better for two isotopes of the same element than for isotopes of different elements. Precision is also better for a continuous sample than for a transient one. The precision is still not as good

as expected from counting statistics, for reasons that are not yet clear. The ion signal is also ~ 100X weaker than would be the case with a single quadrupole device. Possible improvements in these areas are currently being investigated.

ACKNOWLEDGEMENTS

Ames Laboratory is operated for the U. S. Department of Energy by Iowa State University under Contract No. W-7405-ENG-82. This work was supported by the U. S. Department of Energy, Environmental Remediation and Waste Management, Office of Technology Development. Helpful comments from Philip A. Freedman are gratefully acknowledged.

LITERATURE CITED

1. I. Begley and B. L. Sharp, J. Anal. At. Spectrom. 9, 171 (1994).

2. G. P. Russ III, "Isotope Ratio Measrements Using ICP-MS", in *Applications of ICP-MS*, A. R. Date and A. L. Gray, Eds. (Blackie, London, 1989), p. 108.

3. M. Janghorbani and B. T. G. Ting, "Stable Isotope Tracer Applications of ICP-MS", in *Applications of ICP-MS*, A. R. Date and A. L. Gray, Eds. (Blackie, London, 1989), Chap. 5.

4. K. E. Jarvis, A. L. Gray and R. S. Houk, *Handbook of ICP-MS*, (Blackie, London, 1991), pp.225, 235, 312, 326.

5. B. T. G. Ting and M. Janghorbani, Spectrochim. Acta, Part B 42B, 21 (1987).

6. R. E. Serfass, J. J. Thompson and R. S. Houk, Anal. Chim. Acta 188, 73 (1986).

7. E. S. Beary, P. J. Paulsen and J. C. Travis, J. Anal. At. Spectrom., paper submitted (1994).

8. N. Furuta, J. Anal. At. Spectrom. 6, 199 (1991).

9. M. E. Ketterer, M. J. Peters and P. J. Tisdale, J. Anal. At. Spectrom. 6, 439 (1991).

10. P. G. Whittaker, J. F. R. Barrett and J. G. Williams, J. Anal. At. Spectrom. 7, 109 (1992).

11. M. W. Blades and G. Horlick, Spectrochim. Acta, Part B 36B, 861, 881 (1981).

12. N. Furuta and G. Horlick, Spectrochim. Acta, Part B 37B, 53 (1982).

13. S. H. Tan and G. Horlick, J. Anal. At. Spectrom. 2, 745 (1987).

14. S. A. Meyers and D. H. Tracy, Spectrochim. Acta, Part B 38B, 1227 (1983).

15. R. M. Belchamber and G. Horlick, Spectrochim. Acta, Part B 37B, 1037 (1982).

16. J. M. Mermet and J. C. Ivaldi, J. Anal. At. Spectrom. 8, 795 (1993).

17. J. C. Ivaldi and T. W. Barnard, Spectrochim. Acta, Part B 48B, 1265 (1993).

18. J. C. Travis, M. R. Winchester, M. L. Salit, B. J. Wythoff and A. Scheeline, Spectrochim. Acta, Part B 48B, 691 (1993).

19. A. J. Walder, D. Koller, N. M. Reed, R. C. Hutton and P. A. Freedman, J. Anal. At. Spectrom. 8, 1037 (1993).

20. A. J. Walder and N. Furuta, Anal. Sci. (Japan) 9, 675 (1993).

21. A. J. Walder, I. D. Abell, I. Platzner and P. A. Freedman, Spectrochim. Acta, Part B 48B, 397 (1993).

22. V. A. Fassel and B. R. Bear, Spectrochim. Acta, Part B 41B, 1089 (1986).

23. K. W. Olson, W. J. Haas, Jr. and V. A. Fassel, Anal. Chem. 46, 632 (1977).

24. A. L. Gray, R. S. Houk, and J. G. Williams, J. Anal. At. Spectrom. 2, 13 (1987).

25. R. K. Winge, J. S. Crain and R. S. Houk, J. Anal. At. Spectrom. 6, 601 (1991).

26. J. W. Olesik and J. C. Fister III, Spectrochim. Acta, Part B 46B, 851, 869 (1991).

27. S. E. Hobbs and J. W. Olesik, Anal. Chem. 64, 274 (1992).

28. M. T. Cicerone and P. B. Farnsworth Spectrochim. Acta, Part B 44B, 897 (1989).

29. J. A.Olivares and R. S. Houk, Anal. Chem. 57, 2674 (1985).

30. J. Roboz, *Mass Spectrometry Instruments and Techniques* (Wiley, New York, 1986), p. 86.

31. H. E. Duckworth and S. N. Ghoshal, "High Resolution Mass Spectroscopes", in *Mass Spectrometry*, C. A. McDowell, Ed. (McGraw-Hill, New York, 1963), pp. 216-226.

32. H. Wollnik and A. Ewald, Nucl. Instrum. Methods 36, 93 (1965).

33. H. Wollnik, *Optics of Charged Particles*, (Academic Press, Orlando, Florida, 1987), p. 202.

34. P. A. Freedman, personal communication (1994).

35. D. A. Skoog, D. M. West and F. J. Holler, *Fundamentals of Analytical Chemistry,* (Saunders New York, 1988), 5th Ed., p. 38.

36. J. E. Fulford and D. J. Douglas, Appl. Spectrosc. 40, 971 (1986).

37. S. D. Tanner, Spectrochim. Acta, Part B 47B, 809 (1992).

Table I. Instrumental Components and Operating Conditions

COMPONENT	OPERATING CONDITIONS
ICP:	
Continuous flow ultrasonic nebulizer with pumped out drain	Solution uptake 1.9 mL/min Heater temperature 140° C Condenser Temperature 2° C
Plasma Therm generator (now RF Plasma Products) Model HFP-2000 D	Forward power 1.25 kW Reflected power 20 W
RF Plasma Products torchbox (modified in-house for horizontal operation with home-made copper shielding box) with a Matheson mass flow controller for aerosol gas control	Aerosol gas flow 0.9 L/min Outer gas flow 16 L/min Auxillary gas flow 0.8 L/min
Load coil	Homemade three turn coil grounded to shielding box at downstream end using a copper strap
Ion Extraction Interface:	
Ames Laboratory construction	Sampler orifice 1 mm diam. Skimmer orifice 1 mm diam. Sampling position 8 mm from coil on center Sampler-to-skimmer orifice separation 12 mm

Table I (continued)

Vacuum System:

Ames Laboratory
construction; three stage
differentially pumped
welded stainless steel

Differential pumping
aperture dia. 1.5 mm

Operating pressures (torr):

Expansion chamber	1.2
Second stage	6×10^{-4}
Third stage	6×10^{-6}

Mass Analyzers:

VG Plasma Quad components
Model SXP300 quadrupoles
with RF-only pre-filters;

Mean rod bias 0 V

Model SXP 603 Controllers
and RF Generators

Galileo Model 4870 channel
electron multipliers in
pulse counting mode

Bias voltage -2500 V

Counting Electronics:
EG&G ORTEC-

- Model 660 dual 5 kV bias supply
- Model 9302 amplifier/discriminator
- Model 994 dual counter/timer

Table II. Typical Applied Voltages for Ion Lenses and Beam Spitter (see Fig. 1).

Lens	Voltage (V)
Sampler and skimmer	Grounded
1st extraction lens	-180
2nd extraction lens	-22
Diff. pumping aperture	-174
Beam shift plates	-2.7, -0.8, -2.3, -0.8*
Beam splitter center	-70
Beam splitter outside pieces	-83, -85
Beam splitter top plate	+20
Beam splitter bottom plate	-77

	leftside	right side
Fringe field plates	-92	-200
Focusing lenses	-192, -29	-200, -61
Quadrupole entrances	-5.2	-1.8

* Voltages are listed for the four plates shown in the inset ("on-axis view"), in clockwise order beginning at the far left.

Table III. Dimensions of Beam Splitter (see Fig. 2 for explanation of symbols).

Dimension	Symbol	Value (mm)
Overall width	W	120
Height	h	50
Vertical Radii	$R_a = R_b$	200
Horizontal Radii	r_a	179
	r_b	194
Gap between sectors	a	15
Deflection angle	ϕ	30^o

Table IV. Effect of Dwell Time on Precision of Cu Isotope Ratio.

	%RSD of ^{63}Cu / ^{65}Cu Ratio	
Dwell Time (sec)	Measured	Counting Statistics
0.05	2.06	1.5
0.10	1.61	1.1
0.50	0.75	0.49
1.0	0.49	0.35
2.0	0.38	0.25
5.0	1.72	0.16

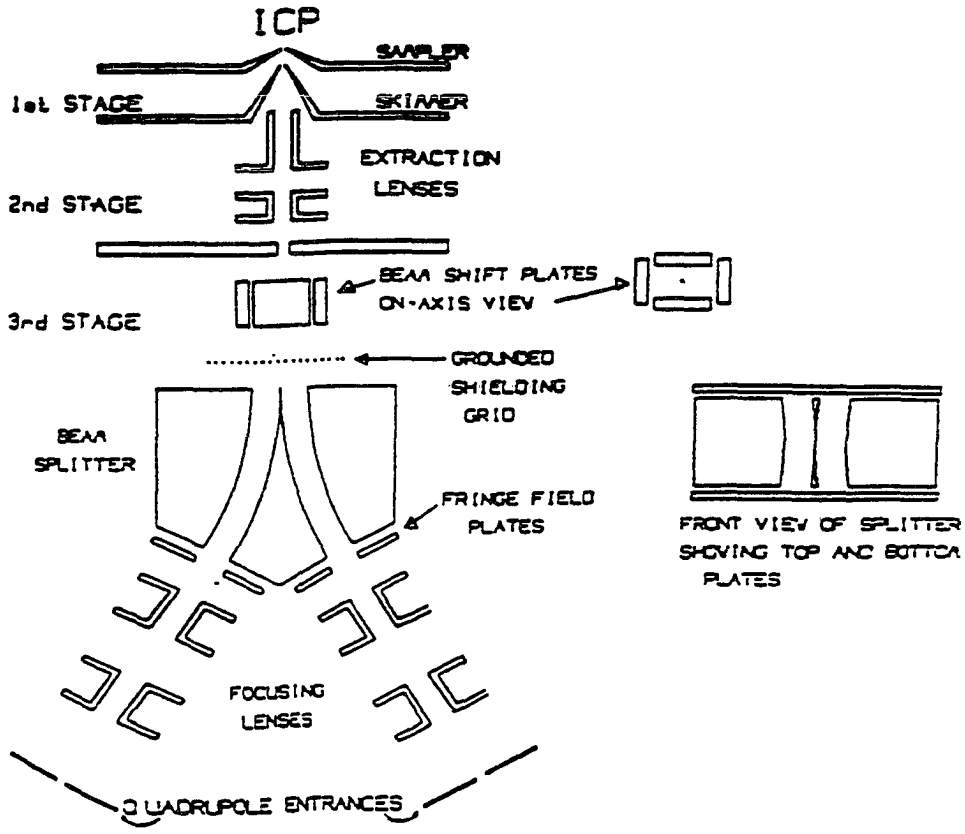

Fig. 1. Extraction system and ion optics for the twin quadrupole device.

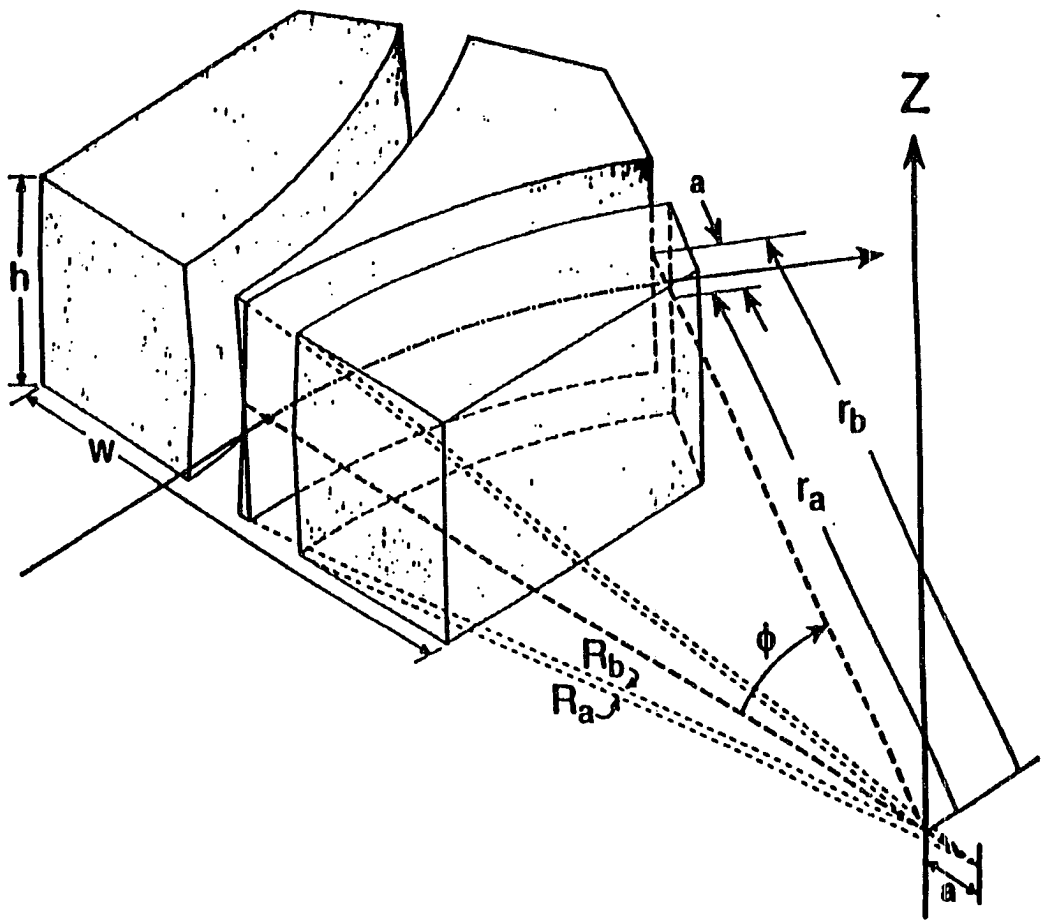

Fig. 2. Beam splitter with top plates, shielding grid, and fringe field plates removed. See Table II for dimensions.

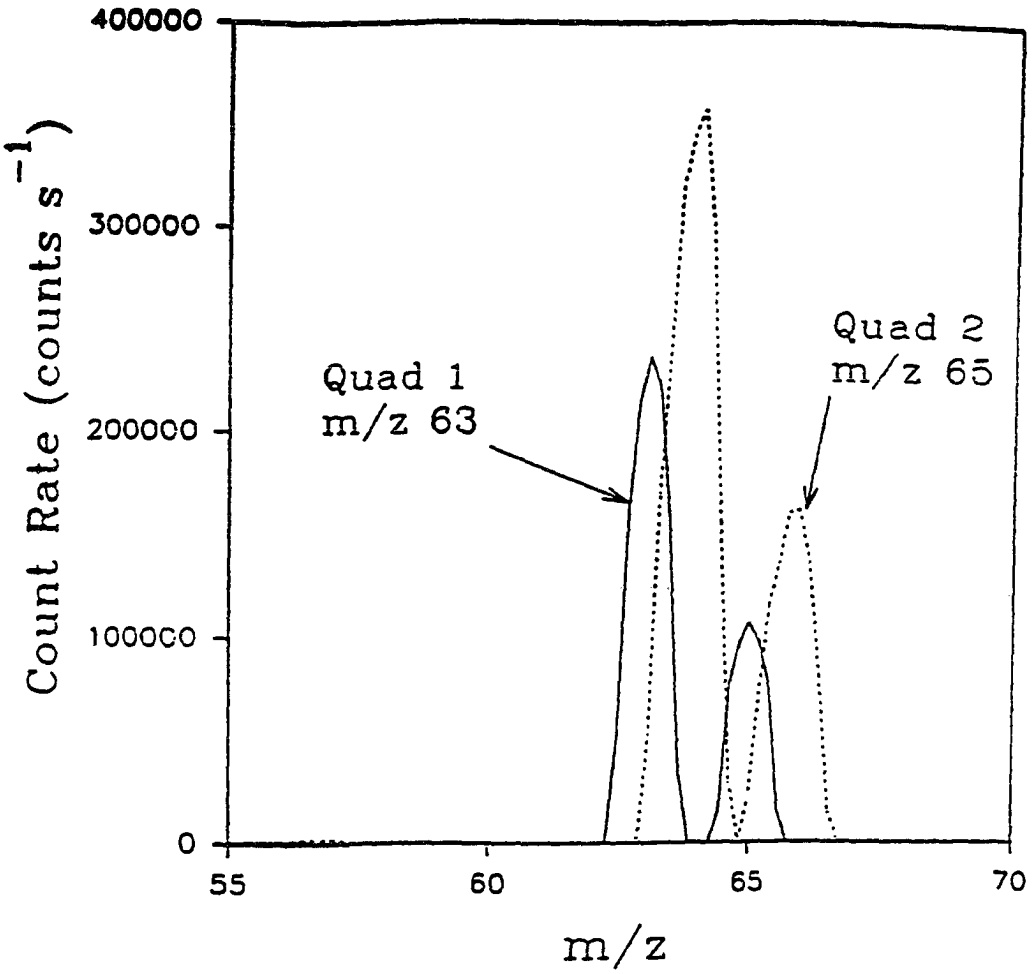

Fig. 3. Mass spectra from both quadrupoles for continuous nebulization of 10 ppm Cu. The spectrum from quad 2 is offset for clarity.

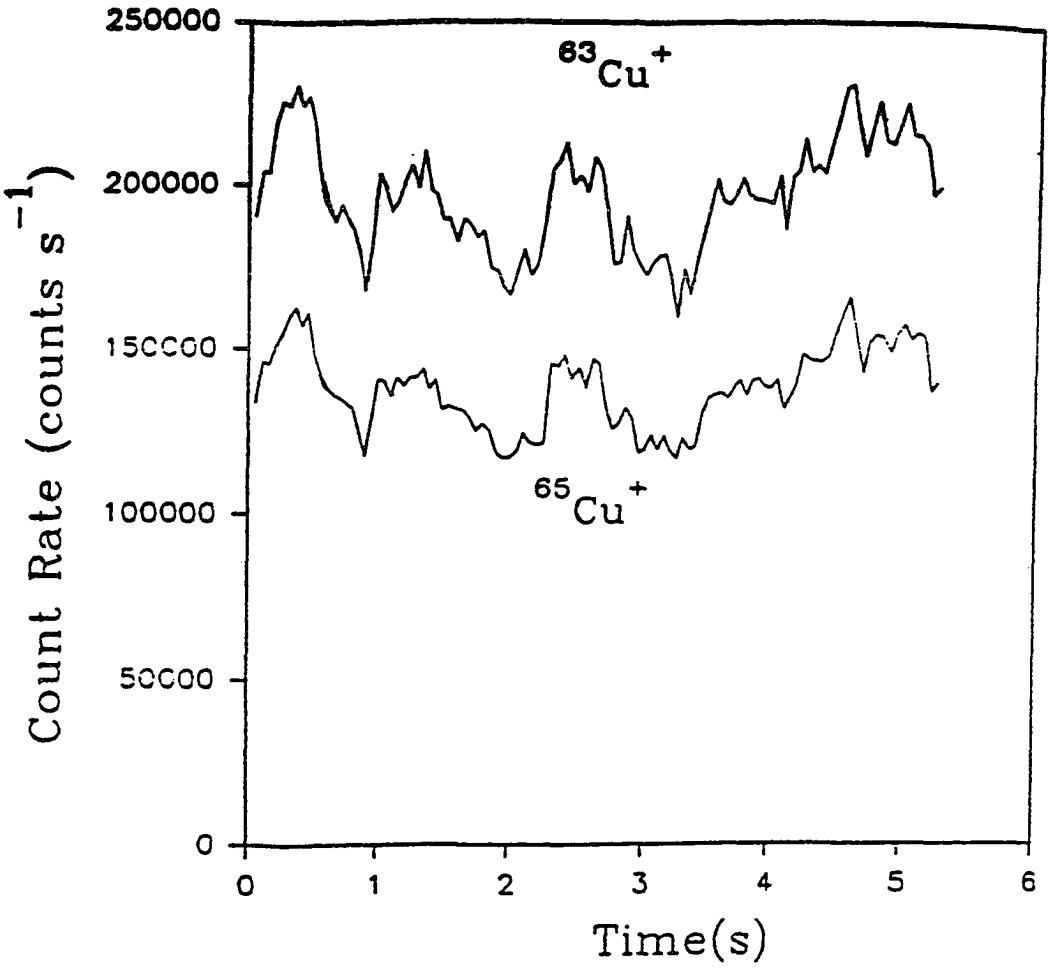

Fig. 4. Plot of count rate vs. time during continuous nebulization of 10 ppm Cu, dwell time = 50 ms. The RSD of each signal is 8.5%, while the RSD of the ratio is 2.0%.

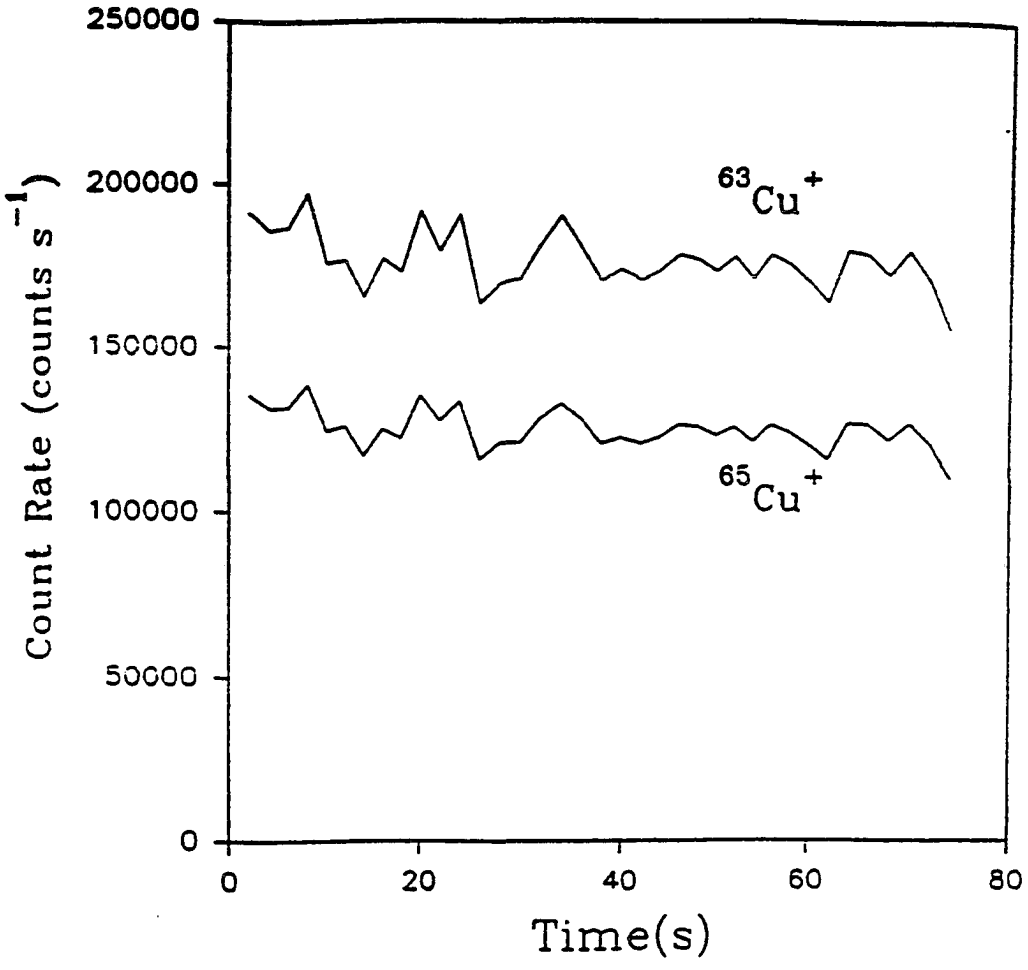

Fig. 5. Plot of count rate vs. time for 10 ppm Cu, dwell time = 2.0 s. The RSD of each signal is 4.5%, while the RSD of the isotope ratio is 0.38%

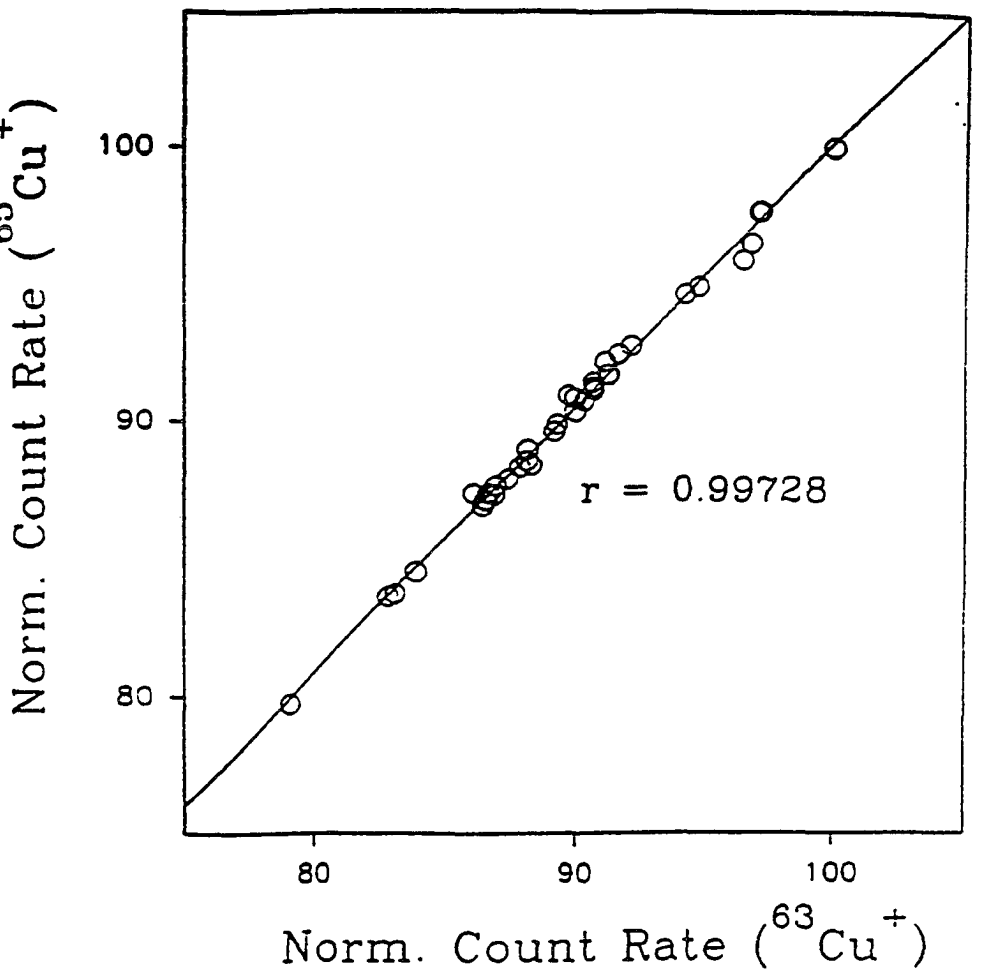

Fig. 6. Correlation plot for copper isotopes, 10 ppm Cu, dwell time = 2.0 s. The correlation coefficient is 0.9973.

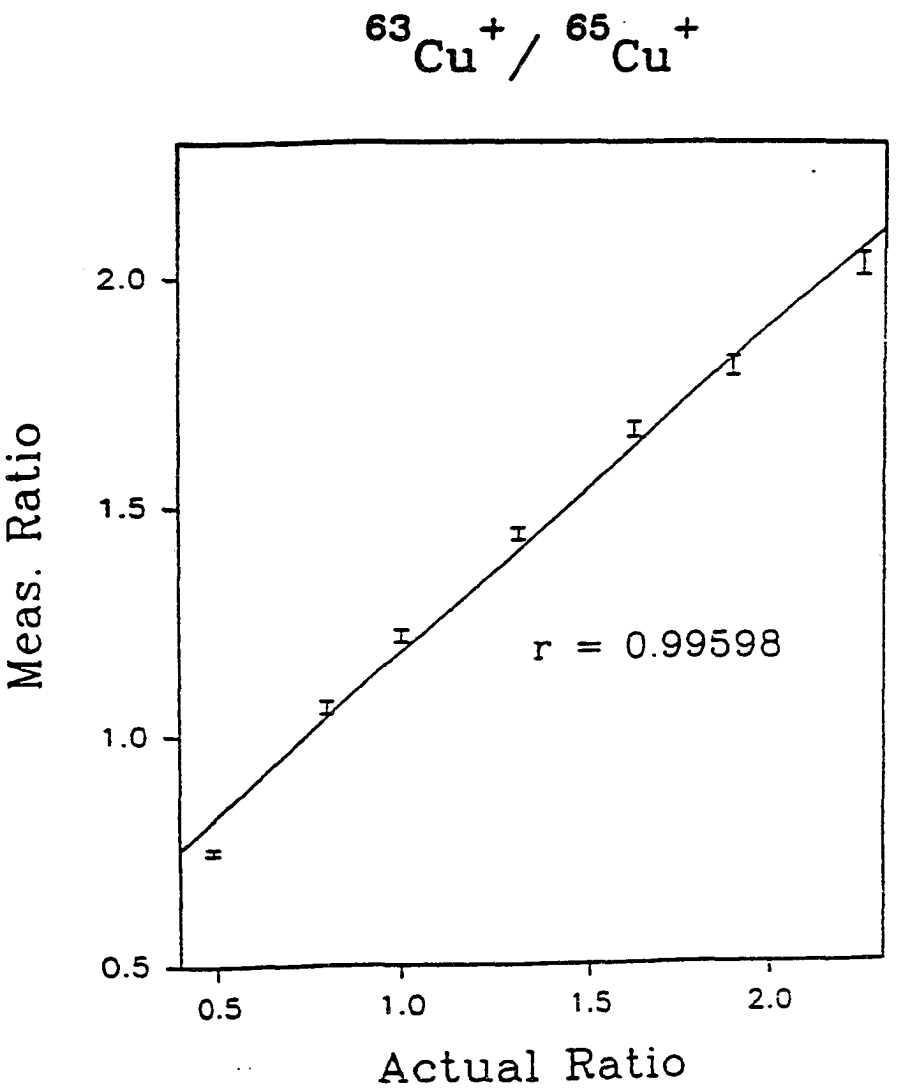

Fig. 7. Calibration plot for mass bias for copper isotope ratios.

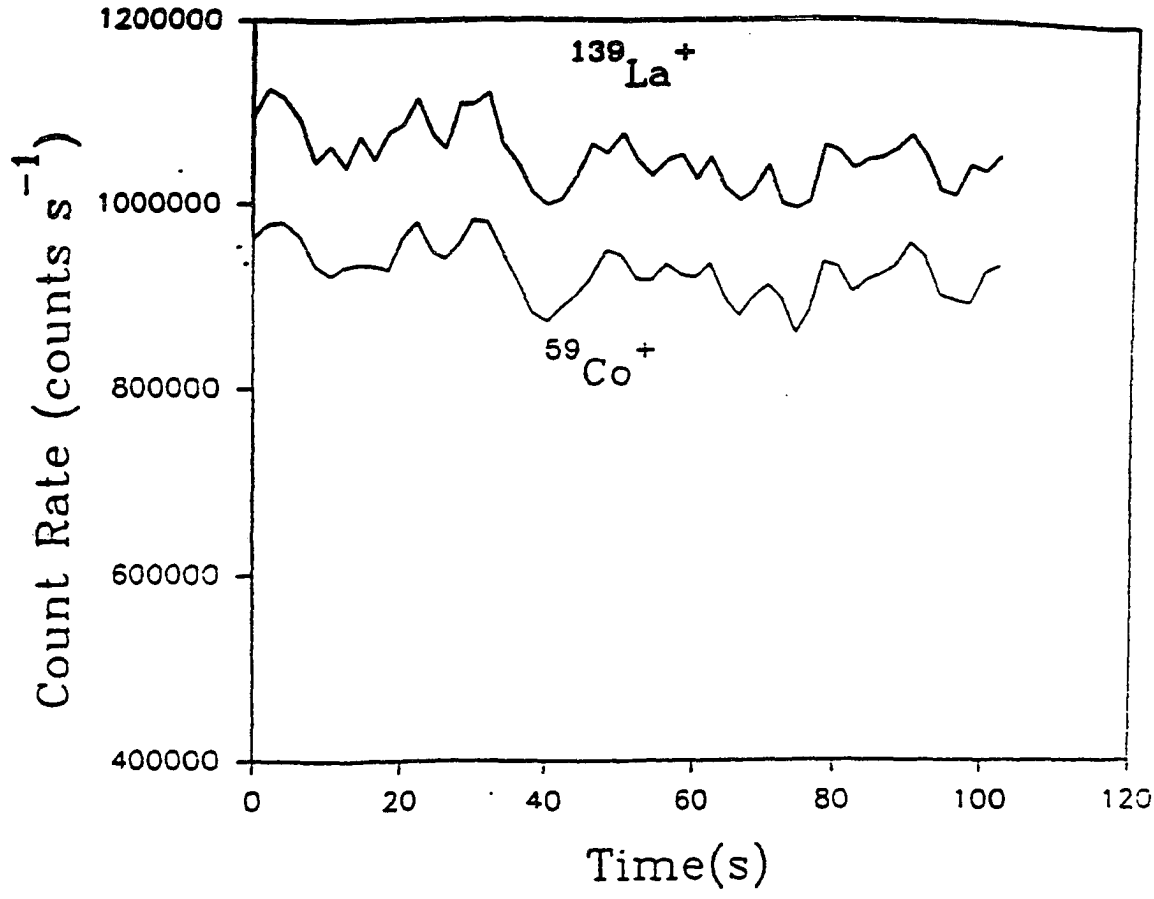

Fig. 8. Plots of signal vs. time for Co^{+} and La^{+}, each at 10 ppm. Dwell time = 2.0 s.

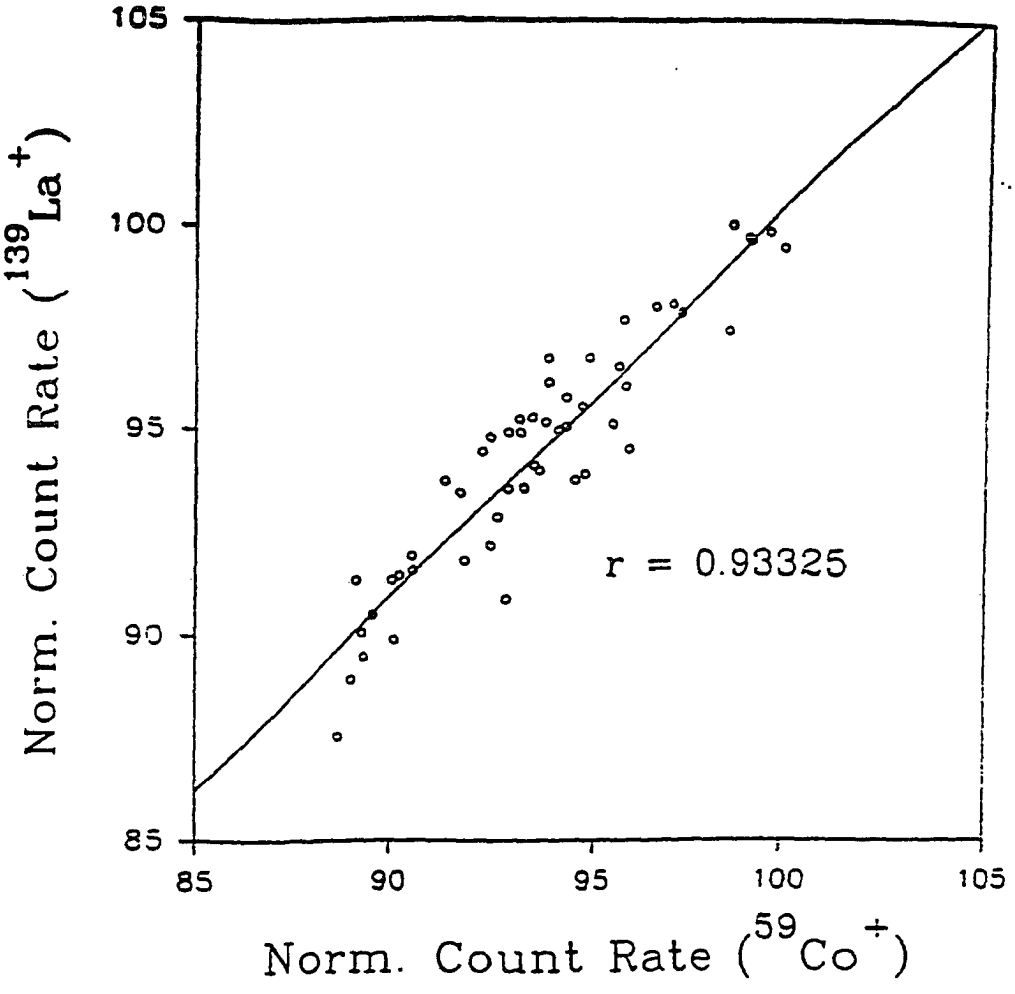

Fig. 9. Correlation plot for La^{+} signal vs. Co^{+} signal. Dwell time = 2.0 s, continuous nebulization of 10 ppm Co and La. The correlation coefficient is 0.9332.

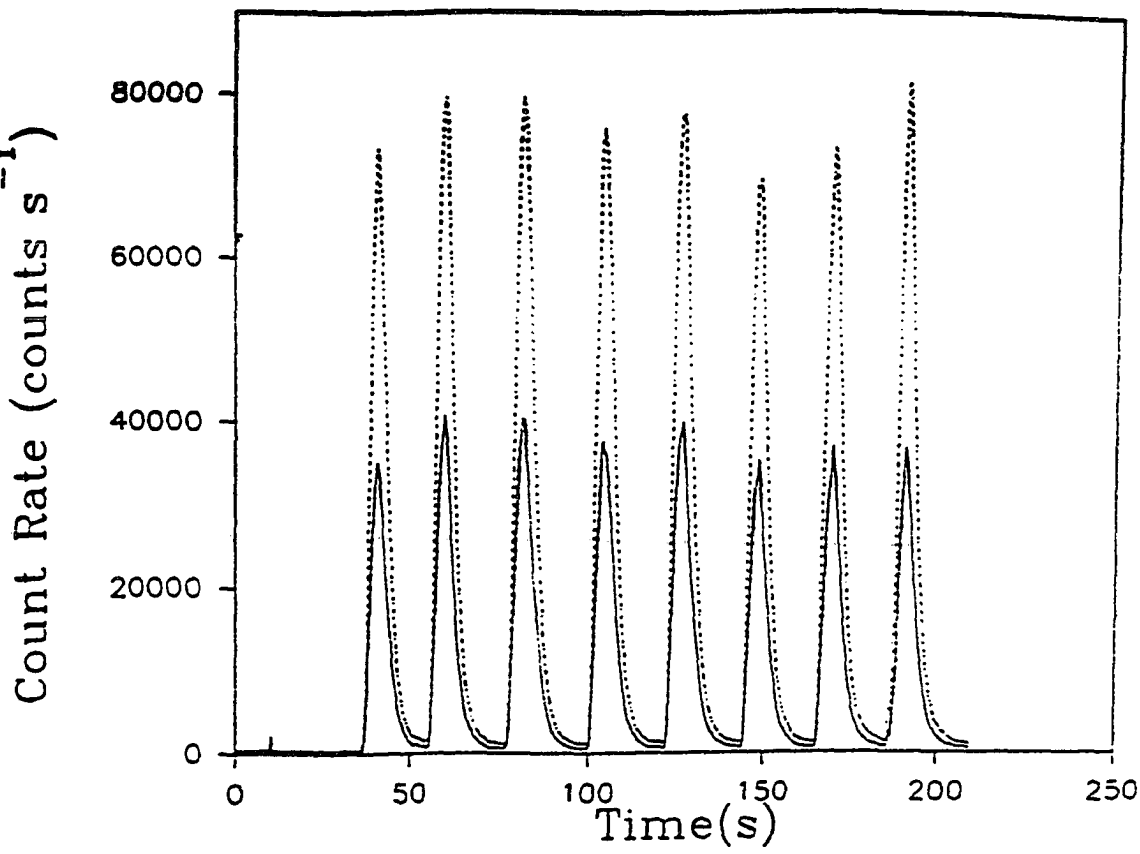

Fig. 10. Flow injection peaks for Cu isotopes, injection volume = 100 μL of 10 ppm Cu, dwell time = 0.3 s. Dotted line : $^{63}Cu^{+}$; solid line : $^{65}Cu^{+}$.

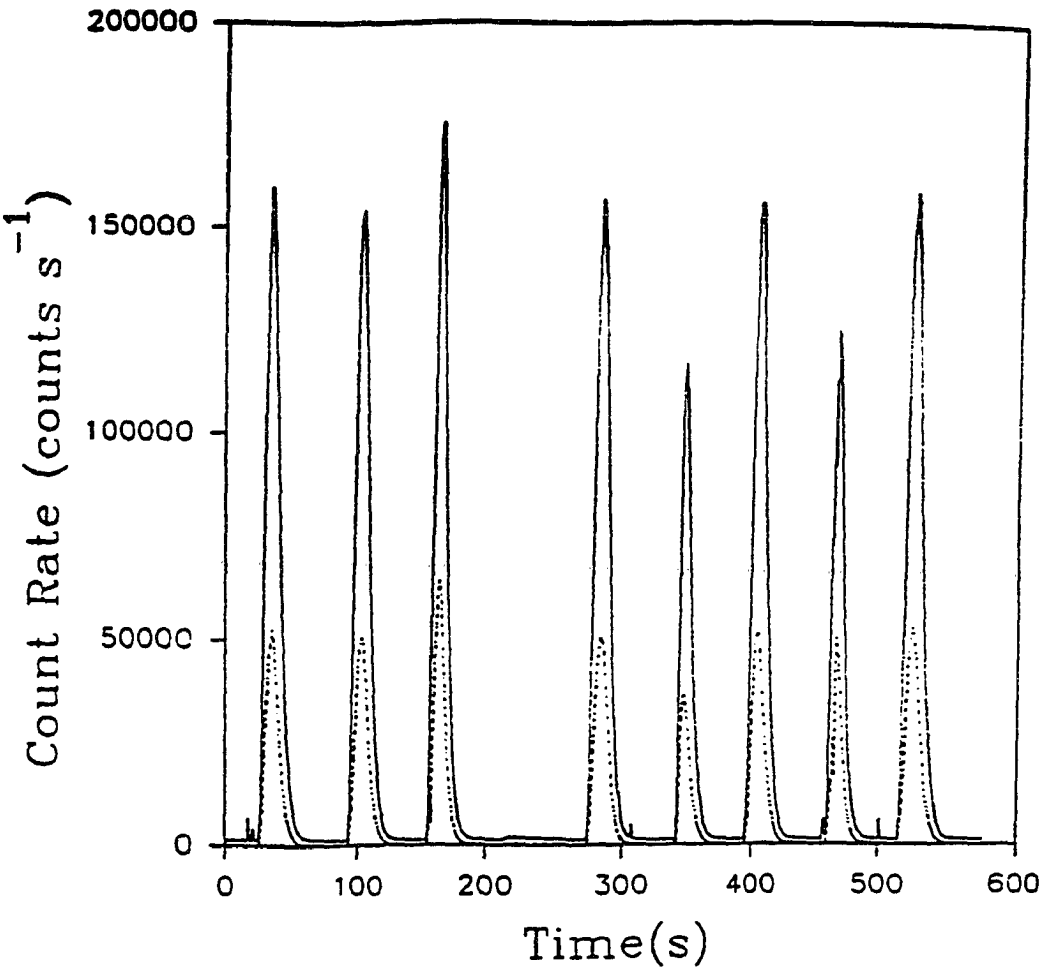

Fig. 11. Flow injection peaks for Co (dotted line) and La (solid line), each at 10 ppm in 250 µL injected. Dwell time = 0.5 sec.

3. THE EFFECT OF A CESIUM MATRIX ON ION RATIOS MEASURED BY INDUCTIVELY COUPLED PLASMA-MASS SPECTROMETRY WITH A TWIN QUADRUPOLE INSTRUMENT

A paper submitted to Applied Spectroscopy

A. R. Warren, L. A. Allen, H-M Pang and R. S. Houk

GENERAL INTRODUCTION

Since the first paper on inductively coupled plasma-mass spectrometry (ICP-MS) was published in 1980 by Houk *et al.* (1), many studies have been reported on the various factors affecting analyte signals (1-9). In ICP-MS, the sample matrix may change the analyte signal intensity. In general, a suppression of analyte signal is observed with increasing concentration of the matrix element, and suppression effects occur to some degree with the addition of almost any matrix element.

Several trends have been observed in studies of the effects of differing matrix elements on analyte ions (6). Heavier concomitant elements cause more suppression than

lighter ones. The degree of ionization of the matrix element also affects suppression, as elements which are more easily ionized create a greater suppression of analytes (5). In addition, lighter mass analytes are suppressed to a greater degree than heavy mass elements (7).

It has also been observed that the extent of the matrix effect depends on the absolute amount of the matrix element, and not the relative amount of matrix to analyte (6). This type of generalized suppression is more severe than that found in ICP-AES (11), and it has been theorized by many that the mass spectrometric system and atmospheric extraction interface must be involved. The matrix effect in ICP-MS seems to be associated with changes in transmission through the interface elements and ion optics preceding the mass spectrometer (4). In the case of an easily ionized concomitant, the increase in ion current can defocus the ion beam by space charge effects, resulting in poorer transmission of analyte ions to the mass analyzer.

The causes of the suppression of the analyte ion have been the subject of many investigations. Two of the most important factors are the atomic mass and the degree of ionization of the concomitant element. Low mass analytes are affected by mass discrimination, both in transmission through the ion optics and in the sampling process itself, as a light ion in a heavier buffer gas of argon will be bounced around

more and consequently is less able to traverse the critical region of the interface. Thus, the greater the mass and the greater the degree of ionization of the concomitant element, the higher the ion currents and the greater the likelihood that matrix ions will displace the analyte ions both in the extraction interface and the ion optics.

Matrix effects can be minimized by adjusting the instrumental parameters, altering the sample introduction methods, or through the chemical separation of the matrix element. Matrix effects may be compensated for by the use of internal standards whose mass and degree of ionization are close to those of the analytes (5). Matrix effects have also been reduced by various modifications of the extraction interface involving the removal of ion lenses in the second expansion stage, changing the diameters of the sampler and skimmer orifices, and placing nonzero potentials on the sampler and skimmer (6, 12-14).

The twin quadrupole device allows the simultaneous acquisition of two different ionic species in the plasma. This property should allow for precise measurements of an analyte and an internal standard element in order to compensate for the matrix supression effect.

EXPERIMENTAL

Twin Quadrupole Instrument

The instrument used for this study has been described previously (10). Two changes were made in the experimental setup: first, an ultrasonic nebulizer which has the spray chamber drain pumped out by a peristaltic pump was used. Second, new detectors were used, both of which were supplied from the same high voltage source, to reduce one more source of noise.

Operating Conditions and Procedures

These are identified in Table I. The voltages applied to the beam splitter were optimized daily with a solution of 1 ppm La until relatively equal count rates were seen in both channels for $^{139}La^{+}$. After this optimization, distilled deionized water was nebulized for 5 minutes before proceeding with the day's experiments. Plasma conditions and lens voltages were then adjusted to provide maximum ion signals for the ions of interest. The sample concentration was typically 1 ppm in 1% HNO_3 in distilled deionized water. This concentration yielded ion count rates in the range of 10^5 counts sec^{-1}, an improvement over the earlier reported performance (10).

Sample solutions were prepared from 1000 ppm single element standards by dilution with 1% HNO_3 in deionized

distilled water. For measuring the matrix effect on ion ratios of differing elements, a stock solution was prepared from the two elements at 250 ppm each, and dilutions were made from this stock solution. A cesium stock solution at 10,000 ppm was diluted with 1% HNO_3 to make up analyte solutions containing either 200 or 500 ppm Cs. The stock solution contained negligible amounts of the analyte elements involved in the study. The dwell time for the ratios was 1 second.

RESULTS AND DISCUSSION

The effect of increasing cesium matrix interference on the ratios $^{115}In/^{115}In$, $^{107}Ag/^{109}Ag$, $^{115}In/^{109}Ag$, and $^{115}In/^{121}Sb$ are shown in Table II along with the ionization energies of the elements involved. Each series of ratios was taken on different days after optimization of the instrumental conditions of that day. The analyte elements were chosen to be similar in mass to each other as well as the concomitant so that mass discrimination effects would not be significant.

Preliminary studies of the matrix effect indicated that for this instrument the suppression of analytes began at a concentration value of ~100 ppm. Solutions of 200 and 500 ppm cesium were deemed sufficient to suppress the analyte signals for matrix effect studies on ion and isotope ratios.

The 'self' ratio for ^{115}In and the silver isotope ratio remain essentially unaffected by increasing matrix concentration. While the signal for each ion is reduced, this effect was equal in both channels. The precision of both ratios is worse by nearly 25% with the Cs matrix present. This worsening of precision may be due in part to the reduction in overall counts brought on by the matrix interference. However, the later studies with more easily suppressed elements result in a similar reduction in precision, so this cannot be the principal reason for the degradation of the precision.

The value of the $^{115}In/^{109}Ag$ ratio increases by approximately 9% with the increase in the cesium matrix, with the majority of the increase coming upon changing to the 200 ppm cesium matrix solution. Silver, with a higher ionization energy (7.5 eV) than indium (5.7 eV), seems to be suppressed to a greater degree, which causes the ratio to go up as indium counts do not suffer the same suppression. The precision of the $^{115}In/^{109}Ag$ ratio is degraded out of proportion to the increased ratio value. This increase in the ratio seems to bear out the trend of greater matrix suppression for an analyte with a lower degree of ionization; however, the worsening of the precision cannot be easily explained

For the ratio $^{115}In/^{121}Sb$, the value of the ratio

increases 51%, a much greater amount than the $^{115}In/^{109}Ag$ ratio. This reflects the fact that antimony, with an even higher ionization energy (8.5 eV) than silver, is suppressed to an even greater degree in the presence of the cesium matrix. The precision of the ratio $^{115}In/^{121}Sb$ decreases by nearly 41%.

CONCLUSIONS

The results of this experiment have shown that for this particular instrument, analytes with higher ionization energies are suppressed to a greater degree in the presence of a matrix element. Since the analytes were chosen to be close in mass to the matrix element, the possibility of mass discrimination effects is negligible. When changes do occur in either the ratio or the precision, the greatest change occurs upon the introduction of the 200 ppm matrix, with a milder change upon switching to the more concentrated cesium solution, which seems to support the use of only two matrix solution concentrations for this experiment.

The worsening of the precision of the ratios upon increasing the matrix concentration seems to give evidence of disturbances in the transmission of analyte ions through the ion optics and the beam splitter. The precision of both the $^{115}In/^{109}Ag$, and $^{115}In/^{121}Sb$ ratios depends on the

consistency of the beam splitting which in turn depends on a homogenous ion beam at the entrance of the splitting element. In every case studied, the precision of the ratio worsens considerably upon introduction of the cesium matrix; we believe that this is indicative of an inhomogenous or unsymmetrical beam, i.e., that the beam shape and/or position depend on the concentration of the matrix element. This inconsistency in ion throughput has been observed by other researchers (6). It is believed that the increase in ion current which occurs with the addition of a relatively easily ionized matrix element disturbs the effective focusing of the ion beam, which is a possible reason why the precision of the ratios $^{115}In/^{115}In$ and $^{107}Ag/^{109}Ag$ also worsens to a degree equal to that of the ion ratios of differing elements with different degrees of ionization.

LITERATURE CITED

1. R. S. Houk, V. A. Fassel, G. D. Flesch, H. J. Svec, A. S. Gray, and C. E. Taylor, Anal. Chem. 52, 2283 (1980).

2. D. J. Douglas and R. S. Houk, Prog. Anal. At. Spectrosc. 8, 1-18 (1985).

3. R. S. Houk and J. J. Thompson, Mass Spectrom. Rev. 7, 425-461 (1988).

4. G. R. Gillson, D. J. Douglas, J. E. Fulford, K. W. Halligan, and S. D. Tanner, Anal. Chem. 60, 1472-1474 (1988).

5. J. A. Olivares and R. S. Houk, Anal. Chem. 58, 20-25 (1986).

6. S. H. Tan and G. Horlick, J. Anal. At. Spectrom. 2, 745-763 (1987).

7. D. C. Gregoire, Spectrochim. Acta 42B, 895-907 (1987).

8. D. Beauchemin, J. W. McLaren, and S. S. Berman, Spectrochim. Acta 42B, 467-490 (1987).

9. Y-S Kim, H. Kawaguchi, T. Tanaka, and A. Mizuike, Spectrochim. Acta 45B, 333-339 (1990).

10. A. R. Warren, L. A. Allen, H-M Pang, R. S. Houk and M. Janghorbani, Appl. Spectrosc. 48, 1360-1366 (1994).

11. K. Lepta, M. Vaughan, and G. Horlick, Spectrochim. Acta 46B, 967-973 (1991).

12. B. S. Ross and G. M. Hieftje, Spectrochim. Acta 46B, 1263 (1991).

13. K. Hu and R. S. Houk, J. Amer. Soc. Mass Spectrom. 4, 28 (1993).

14. J. S. Crain, R. S. Houk and F. G. Smith, Spectrochim Acta 43B, 1355 (1988).

Table I. Instrumental Components and Operating Conditions

COMPONENT	OPERATING CONDITIONS
ICP:	
Continuous flow ultrasonic nebulizer with pumped out drain	Solution uptake 1.9 mL/min Heater temperature 140° C Condenser Temperature 5° C
Plasma Therm generator (now RF Plasma Products) Model HFP-2000 D	Forward power 1.25 kW Reflected power 15 W
RF Plasma Products torchbox (modified in-house for horizontal operation with home-made copper shielding box) with a Matheson mass flow controller for aerosol gas control	Aerosol gas flow 0.9 L/min Outer gas flow 14 L/min Auxillary gas flow 0.7 L/min
Load coil	Homemade three turn coil
Ion Extraction Interface:	
Ames Laboratory construction	Sampler orifice 1 mm diam. Skimmer orifice 1 mm diam. Sampling position 7 mm from coil on center Sampler-to-skimmer orifice separation 12 mm

Table I (continued)

Vacuum System:

Ames Laboratory construction; three stage differentially pumped welded stainless steel	Differential pumping aperture dia. 1.5 mm Operating pressures (torr): Expansion chamber 1.2 Second stage 6×10^{-4} Third stage 6×10^{-6}
Mass Analyzers: VG Plasma Quad components Model SXP300 quadrupoles with RF-only pre-filters;	Mean rod bias 5 V
Model SXP 603 Controllers and RF Generators	
Galileo Model 4870 channel electron multipliers in pulse counting mode	Bias voltage -2800 V

Counting Electronics:
EG&G ORTEC-
- Model 660 dual 5 kV bias supply
- Model 9302 amplifier/discriminator
- Model 994 dual counter/timer

TABLE II - Matrix effect on ion and isotope ratios

(analyte concentrations at a concentration of 1 ppm)

[Cs]ppm	counts/sec	%RSD of signal	Ratio Avg.	%RSD Ratio
$^{115}In/^{115}In$				
0	334124/316465	10.239/10.083	1.0558	0.9917
200	281190/266253	8.163/7.933	1.0561	0.9976
500	219447/207790	8.333/8.127	1.0561	1.1017
$^{107}Ag/^{109}Ag$				
0	189881/182910	4.349/3.282	1.0378	1.7366
200	141224/136096	8.473/8.085	1.0376	2.2579
500	172024/165711	5.283/4.626	1.0381	2.4177
$^{115}In/^{109}Ag$				
0	343829/165711	10.608/10.873	2.0755	1.1551
200	272372/122328	4.647/4.831	2.2270	1.4956
500	211565/93993	7.353/7.199	2.2502	1.6463
$^{115}In/^{121}Sb$				
0	321899/122938	2.727/2.403	2.6183	0.7488
200	292475/87711	1.991/1.671	3.3345	0.9992
500	227822/57524	2.819/2.714	3.9605	1.0626

4. CORRELATION STUDIES OF THE BEHAVIOR OF SINGLY CHARGED AND DOUBLY CHARGED ATOMIC IONS AND METAL OXIDE IONS IN ICP-MS WITH A TWIN QUADRUPOLE INSTRUMENT

A paper submitted to Applied Spectroscopy

A. R. Warren, L. A. Allen and R. S. Houk

INTRODUCTION

Inductively coupled plasma-mass spectrometry (ICP-MS) is a sensitive and selective technique for trace multielemental analysis. The ICP generates a majority of singly-charged ions which are extracted and introduced into a mass spectrometer for measurement. For a large number of elements the singly charged analyte ion M^+ is not the only analyte species. A number of elements form monoxide species, MO^+, and many form doubly charged ions, M^{2+}.

The occurrence and abundance of these species have been studied by a number of researchers. Houk *et al* (1) observed

spectra of Sr^{2+}, $SrOH^+$, Ba^{2+}, and $BaOH^+$ in studies of Saha-type ionization reactions for the ICP. Houk and Thompson (2) reported seeing strontium, praseodymium, and uranium species, and discussed the formation of oxide and hydroxide species in general. Date and Gray (3,4) reported observing many of these species and the formation of rare earth oxides. Horlick *et al* (5) discussed the behavior of Sr^{2+}, Ba^{2+}, MoO^+, WO^+, and CeO^+ with power and nebulizer flow rate. Douglas and Houk (6) measured ThO^+/Th^+, Ba^{2+}/Ba^+, and UO^+/U^+ ratios, discussed the potential of oxide interferences in ICP-MS, and suggested cerium as one of the worst case analytes for oxide formation. Vaughan and Horlick (7) have tabulated the oxide, hydroxide, and doubly-charged species for most elements and discussed the various effects that plasma conditions can have on their abundances.

The above mentioned analyte species are important in ICP-MS because they may cause spectral interferences with other analyte elements, especially in the case of a matrix oxide interfering with a trace analyte at the same mass. For example, the oxide species of zirconium and molybdenum interfere with the measurement of cadmium isotopes, if these elements are found together in a sample. In addition to the effect of giving a falsely high signal at a particular mass, these spectral overlaps can interfere with isobaric corrections. An isobaric correction involves measuring an

interference-free isotope of an element which has an isotope interfering with the analyte. For example, the contribution of $^{112}Sn^+$ on $^{112}Cd^+$ can be calculated by measuring the count rate of interference-free $^{118}Sn^+$ and calculating the counts for $^{112}Sn^+$ from the known natural abundances of tin isotopes. However, $^{96}MoO^+$ also overlaps at m/z 112, which can cause an error in the analysis. While high resolution ICP-MS instruments are able to resolve and separate many of these overlaps, the majority of ICP-MS instruments use quadrupole mass analyzers, which simply do not have the resolution to distinguish chemically different ions at the same nominal *m/z* value. Thus, for the typical laboratory analyst, a study of the behavior and effects of these analyte species is important. For sensitivity measurements, it is best if the analyte is all in one form, the singly charged elemental ion, M+. The formation of other species is detrimental to analyte sensitivity.

The study of these species is also a concern of fundamental diagnostics of the plasma itself. Investigations into species distribution may tell us if the M^{2+}/M^+ and MO^+/M^+ ratios represent the actual state of the plasma, or whether the ratios are altered through the sampling process. The characterization of analyte ion species distribution in the ICP by ICP-MS may provide more answers.

In this research, the distribution of cerium species

are reported as a function of aerosol flow rate. The twin quadrupole instrument was used to measure the ratios Ce^{2+}/Ce^{+}, CeO^{+}/Ce^{+}, and Ce^{2+}/CeO^{+} as a function of aerosol flow rate, and the correlation of the signals in these ratios was studied.

The use of cross-correlation factors in the study of emission line ratios has been examined by Mermet and Ivaldi using inductively coupled plasma-atomic emission spectroscopy (ICP-AES) with an echelle spectrometer to simultaneously examine two atomic lines through the use of different orders of the echelle grating (9). Flicker noise in the plasma was highly correlated. We have observed the same kind of correlation in the measurement of isotope ratios and internal standard ratios with the twin quadrupole instrument (8). On the other hand, the emission research showed that shot-noise limited signals are uncorrelated.

In ICP-MS, analyte signals may fluctuate due to the incomplete atomization of intact droplets and particles (10). This fluctuation may affect the apparent correlation of analyte signals.

EXPERIMENTAL

The twin-quadrupole device used in this experiment has been previously described (8). The operating conditions are

described in Table I. Before beginning the flow rate studies, the ion lenses were optimized on ^{140}Ce at a flow rate of 0.9 L/min. The 1 ppm cerium solution used for these experiments was prepared by diluting a 1000 ppm cerium standard (Plasma-Chem Industries) with 1% HNO_3 in distilled deionized water. The aerosol gas flow rate was controlled precisely by a mass flow controller calibrated for argon. The power setting and sampling depth remained constant for all observations. For ratio measurements, each quadrupole mass filter was individually set to pass only the species of interest; scanning or peak-hopping was not used. A software program written in-house was used to collect the signals from each ratio, while spreadsheet software (Microsoft Excel) was used for statistical calculations. Each series of ratios at a specific flow rate was collected by changing the mass settings of the quadrupoles and taking all ratio measurements before changing the flow to the next highest rate. The flow was allowed to stabilize for one minute after changing to a higher setting before data were collected.

RESULTS AND DISCUSSION

Parameter Behavior Plots

Plots of count rate vs. aerosol flow for Ce^+, CeO^+, and Ce^{2+} at a power setting of 1.25 kW are shown in Figs. 1-3.

These curves are sometimes called parameter behavior plots. The data shown for cerium follow a pattern which is typical of most analytes. There is an optimum aerosol flow rate which maximizes the signal for each kind of ion. The order in which the signal for the various species reaches a maximum follows a trend in behavior similar to that described for barium species by Vaughan and Horlick (7). For our homemade instrument, the optimum flow rates for each species are very close to each other, as can be seen in the normalized plot in Fig. 4. The doubly-charged cerium ion appears at the lowest flow rate, where the plasma is hotter. The higher temperatures involved should favor the Ce^{2+} ion. The Ce^{+} signal reaches its maximum next, as the higher flow rate cools the plasma somewhat. Finally the signal for CeO^{+} is maximized at slightly higher flow rates which create a cooler plasma that allows molecular species to remain intact through the sampling process. The signal profiles over a range of flow rates are broad, because the nebulizer produces analyte droplets in a wide range of sizes.

Correlation Studies

A plot of the cross-correlation factors for three sets of cerium species ratios is shown in Fig. 5. The cross-correlation factors (r) are also plotted versus aerosol gas flow rate to facilitate comparison with the parameter behavior

plots in Fig. 4. First, consider the region at low aerosol gas flow rate labelled A in Figs. 4 and 5. The signals for all three species show the same trend in this region; they all increase with aerosol gas flow rate (Fig.4). Thus, their signals should behave in a common fashion for aerosol gas flow rates in region A. Fig. 5 shows that these signals are indeed weakly correlated, with positive correlation factors of r ~0.4 to 0.7.

Next, consider region B, where the signal for Ce^{+} is maximized. The correlation coefficient between Ce^{+2} and CeO^{+} is ~ -0.6, i.e., Ce^{+2} and CeO^{+} are anticorrelated to some extent at this aerosol gas flow rate (0.9 L min^{-1}). Here the parameter behavior plot shows that the Ce^{+2} signal decreases with aerosol gas flow rate, while the CeO^{+} signal increases as the aerosol gas flow rate increases. Thus, these two signals respond in different directions to a fluctuation in aerosol gas flow rate, so their signals are nearly anticorrelated. Signals for Ce^{+} and CeO^{+}, and Ce^{+2} and Ce^{+} are essentially uncorrelated in region B (r~0).

Next, consider correlation behavior at high aerosol gas flow rate (>1 L min^{-1}) in region C. In this region, correlation coefficients for Ce^{+} and CeO^{+} are ~0.9. These two signals thus approach correlation. This behavior is expected because the parameter behavior plots show that the Ce^{+} and CeO^{+} signals both decrease as aerosol gas flow rate increases

in region C. The signals for all species decline sharply as aerosol gas flow rate increases in this regime. This decline reduces the number of ions detected and increases the contrubution of shot noise, which limits the quality of the correlation. Hence, only weak correlations are seen between the pairs (Ce^{+2} and Ce^{+}) and (Ce^{+2} and CeO^{+}) at high aerosol gas flow rates.

Finally, correlation coefficients between atomic ions in both channels of the twin quadrupole instrument are essentially unity (8). Thus, a pair of unipositive atomic ion signals is much more closely correlated than any combination of Ce^{+}, Ce^{+2} and CeO^{+} seen in this study.

CONCLUSIONS

The signal maxima for cerium species vs. aerosol flow rate follow the expected pattern which was observed by Vaughan and Horlick (7). The correlation of the ratios of the cerium species is not as great as seen before with the isotopic ratios and internal standard ratios of singly-charged ions; the low signals seen for Ce^{+2} and CeO^{+} makes them susceptible to shot noise interference. These spectral interferences from analyte species will continue to be a problem in ICP-MS for some time to come.

LITERATURE CITED

1. R. S. Houk, H. J. Svec, and V. A. Fassel, Appl. Spectrosc. 35, 380 (1981).

2. R. S. Houk and J. J. Thompson, American Mineralogist 67, 238 (1982).

3. A. R. Date and A. L. Gray, Analyst 108, 1033 (1983).

4. A. R. Date and A. L. Gray, Spectrochim. Acta 40B, 115 (1985).

5. G. Horlick, S. H. Tan, M. A. Vaughan and C. A. Rose, Spectrochim. Acta 40B, 1985.

6. D. J. Douglas and R. S. Houk, Prog. Anal. At. Spectrosc. 8, 1-18 (1985).

7. M. A. Vaughan and G. Horlick, Appl. Spectrosc. 40, 434 (1986).

8. A. R. Warren, L. A. Allen, H-M Pang, R. S. Houk, and M. Janghorbani, Appl. Spectrosc. 48, 1360 (1994).

9. J. M. Mermet and J. C. Ivaldi, J. Anal. Atomic Spectrom. 8, 795 (1993).

10. R. K. Winge, J. S. Crain and R. S. Houk, J. Anal. At. Spectrom. 6, 601 (1991).

11. J. W. Olesik and J. C. Fister III, Spectrochim Acta 46B, 851-869 (1991).

Table I. Instrumental Components and Operating Conditions

COMPONENT	OPERATING CONDITIONS
ICP:	
Continuous flow ultrasonic nebulizer with pumped out drain	Solution uptake 1.9 mL/min Heater temperature 140° C Condenser Temperature 5° C
Plasma Therm generator (now RF Plasma Products) Model HFP-2000 D	Forward power 1.25 kW Reflected power 15 W
RF Plasma Products torchbox (modified in-house for horizontal operation with home-made copper shielding box) with a Matheson mass flow controller for aerosol gas control	Aerosol gas flow variable Outer gas flow 14 L/min Auxillary gas flow 0.7 L/min
Load coil	Homemade three turn coil
Ion Extraction Interface:	
Ames Laboratory construction	Sampler orifice 1 mm diam. Skimmer orifice 1 mm diam. Sampling position 10 mm from coil on center Sampler-skimmer separation 12 mm

Vacuum System:

Ames Laboratory
construction; three stage
differentially pumped;
welded stainless steel

Differential pumping
aperture dia. 1.5 mm

Operating pressures (torr):
Expansion chamber 1.2
Second stage 6×10^{-4}
Third stage 6×10^{-6}

Mass Analyzers:
VG Plasma Quad components
Model SXP300 quadrupoles
with RF-only pre-filters;

Mean rod bias 5 V

Model SXP 603 Controllers
and RF Generators

Galileo Model 4870 channel
electron multipliers in
pulse counting mode

Bias voltage -2800 V

Counting Electronics:
EG&G ORTEC-
- Model 660 dual 5 kV bias supply
- Model 9302 amplifier/discriminator
- Model 994 dual counter/timer

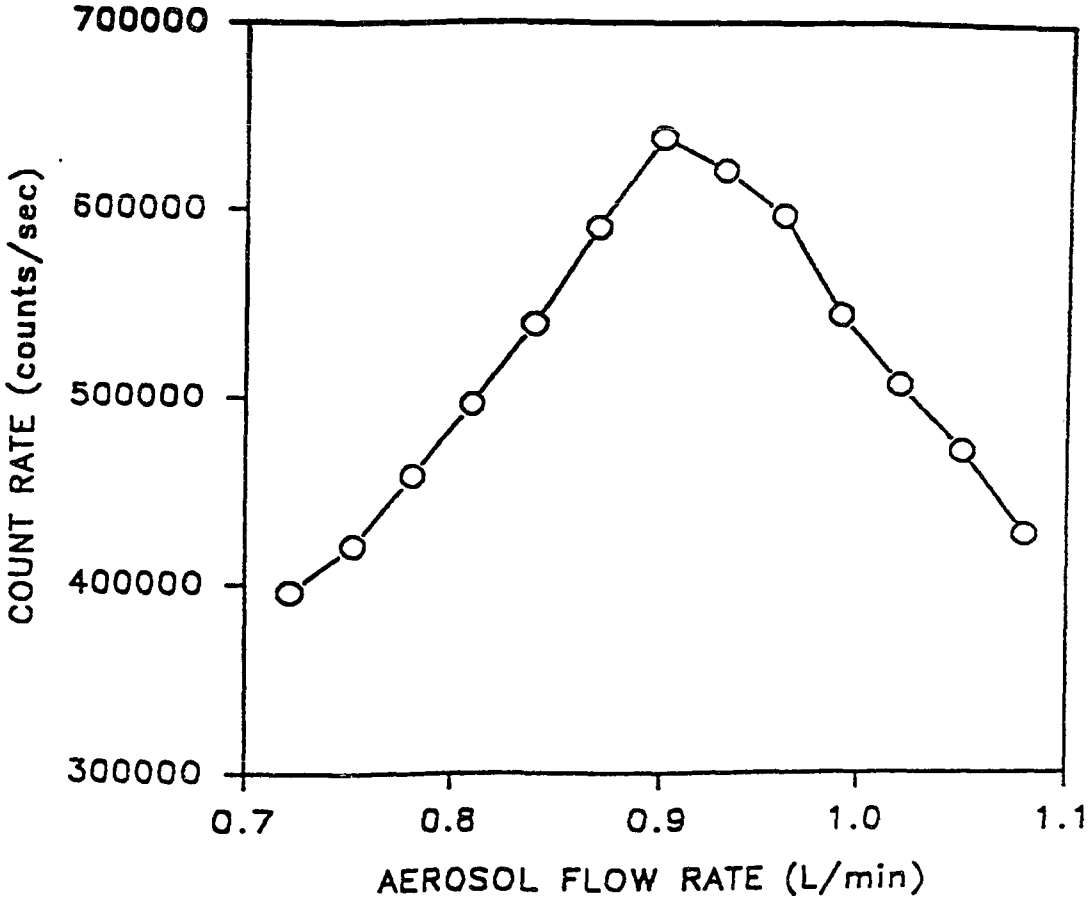

Fig. 1. Dependence of Ce^+ count rate on aerosol gas flow.

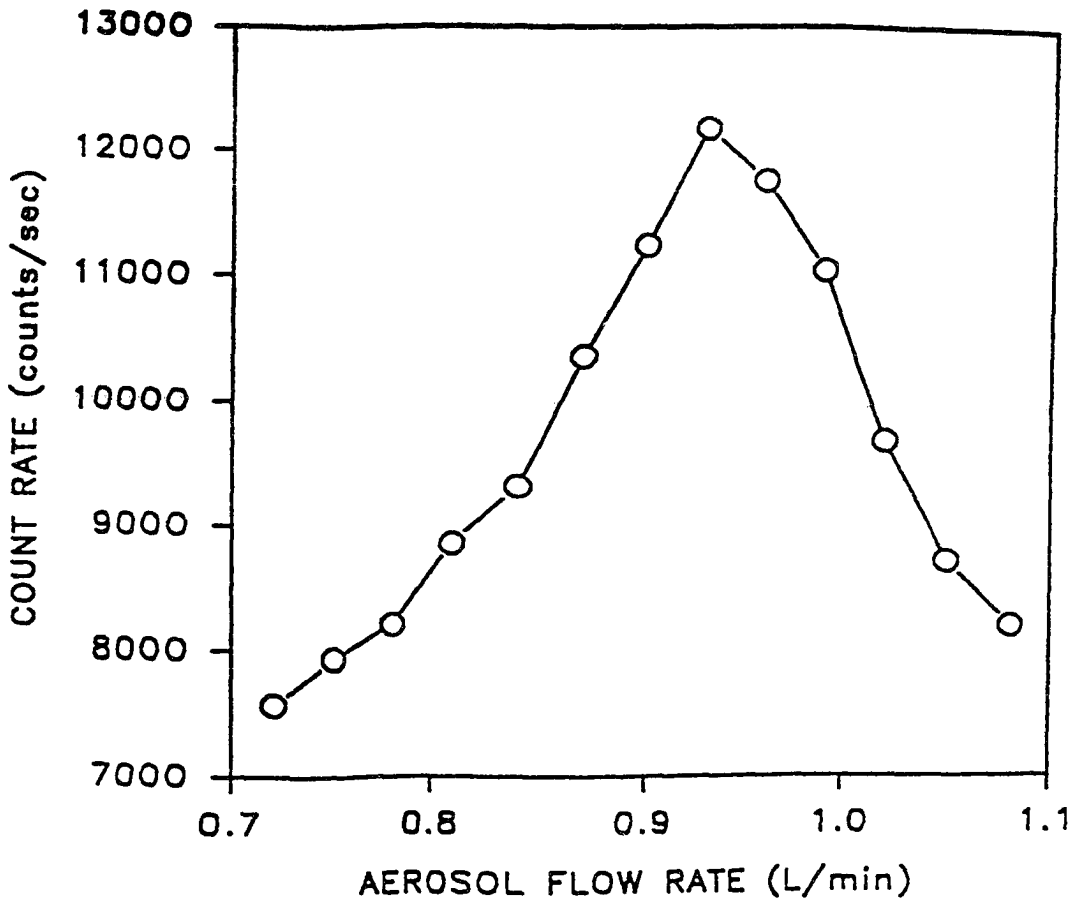

Fig. 2. Dependence of CeO^+ count rate on aerosol gas flow.

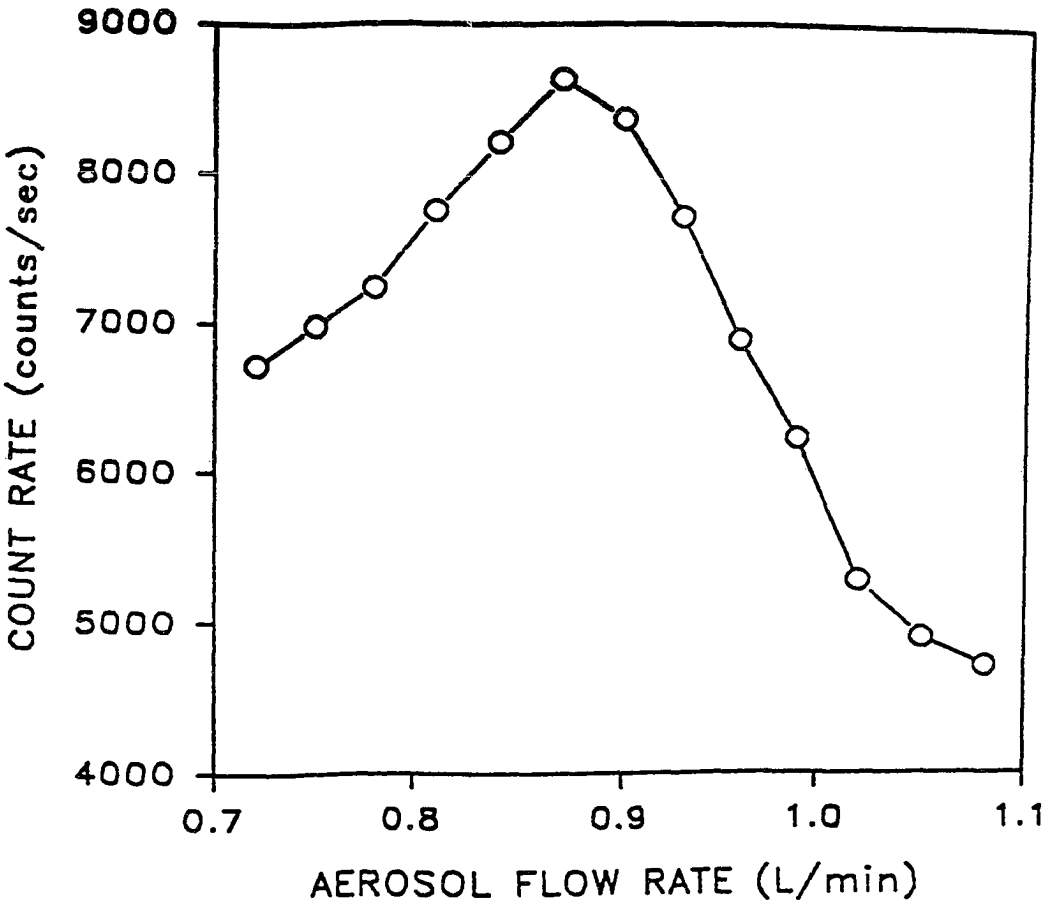

Fig. 3. Dependence of Ce^{2+} count rate on aerosol gas flow.

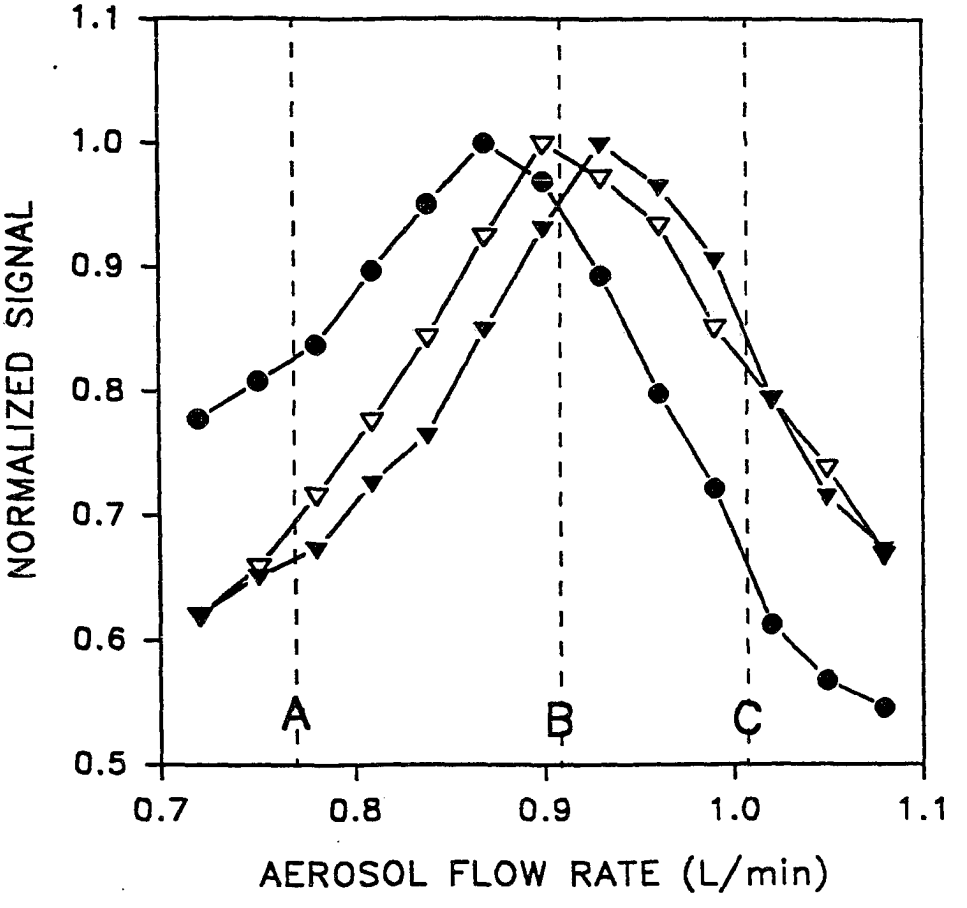

Fig. 4. Change in ion signal vs. aerosol gas flow rate for Ce^{+}(▽), CeO^{+}(▼), and Ce^{2+}(●).

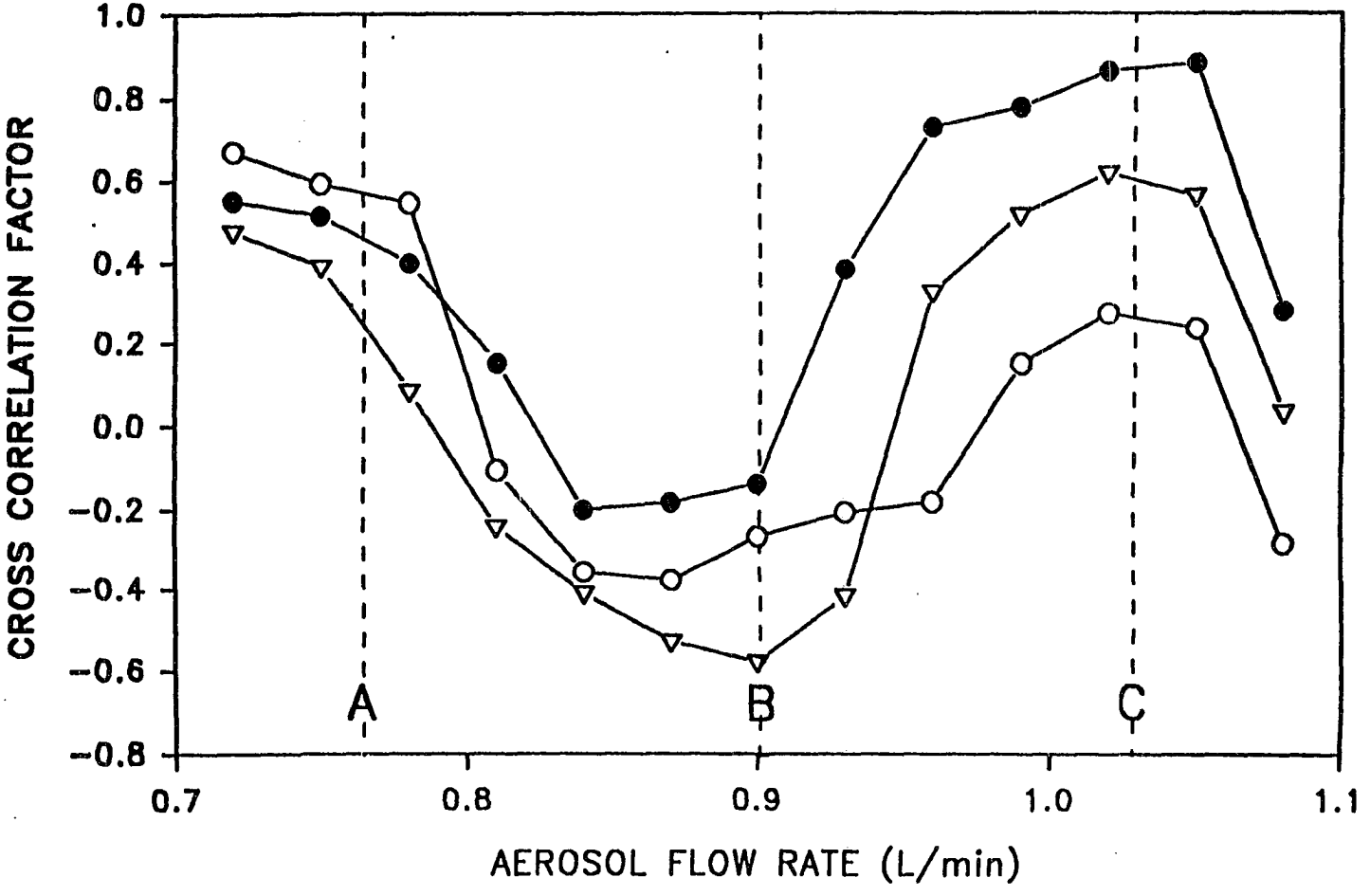

Fig. 5. Cross-correlation of ion ratios vs. aerosol gas flow for Ce^{2+}/Ce^{+} (○), CeO^{+}/Ce^{+} (●), and CeO^{+}/Ce^{2+} (▽).

GENERAL CONCLUSIONS

The results of these experiments indicate the basic feasibility of improving precision by using two quadrupoles to measure two different *m/z* signals simultaneously. Flicker noise in the plasma is effectively cancelled for isotope ratios and reduced for internal standard ratios. Precision is better for continuous signals than transient ones. Analyte signals with very low count rates which are shot-noise limited show little improvement in precision.

The precisions obtained by this unique instrument are, however, still not as good as would be predicted by counting statistics. One possible reason is the nature of the electrostatic beam splitter. While the central element of the beam splitter is razor sharp, the repelling field produced is not. This 'blunt' splitter is probably also responsible for the ~100x weaker ion signal than expected from a conventional ICP-MS instrument. The presence of space charge expansion of the beam in the region in front of the splitter may result in an asymmetrical beam cross section and a resultant uneven splitting. A third reason for less than perfect splitting is possible inhomogeneity of the beam caused by incompletely atomized particles which would create pockets of concentrated analyte ions.

External sources of noise are also a deterrent to improved precision with the twin-quadrupole instrument. RF energies produced by the plasma itself interfere with many

aspects of the experiment. At RF frequencies, nearly every conductor in the laboratory becomes an antenna or reflector of RF energy, which interferes with the data transmission lines and, it is suspected, the power supplies on the ion lenses and splitter within the instrument itself. Inherent noise in the channel electron multipliers is another possible cause of the degradation of ratio precision. Studies done by Freedman, Walder, and co-workers on the double-focusing ICP-MS instrument, where the faraday cups were replaced by channeltron detectors, showed a mediocre ratio precision of ~0.1% RSD. Finally, the low count rates seen for trace level analytes are shot-noise limited, and their precision cannot be improved through the elimination of flicker noise in the plasma.

Another significant problem encountered in this project is the fact that mass peaks generated by quadrupoles are triangular in shape and do not have the flat-topped profile of peaks generated using a sector instrument. Consequently, the mass window in which the counts for each isotope are collected is relatively narrow and difficult to pinpoint precisely.

The reduction of ion throughput also has several possible causes. The nature of the electrostatic fields in front of the splitter may deflect many of the analyte ions from the optimum entrance axes of the two electrostatic deflectors. The long path which the ions traverse through the instrument to the quadrupole entrances may also result

in the loss of ions through space charge repulsion. The focusing action of the splitter elements is not as effective as the double focusing of, for example, a Nier-Johnson geometry in a sector mass spectrometer.

In conclusion, while the instrument has demonstrated the basic feasibility of simultaneous ion measurement for improving the precision of ion ratios, is has not improved them to a degree to make the production and use of such and instrument worthwhile. Furthermore, the capabilities of the double-focusing multicollector ICP-MS instrument eclipse the twin quadrupole device in every way but size and cost.

ACKNOWLEDGEMENTS

My sincerest gratitude and respect to Dr. Sam Houk for guidance, friendship, and his understanding of a non-traditional (i.e., older) grad student. I came to this university to work with this man specifically, and he has given me not only a deep understanding of ICP-MS, but of the nature of chemical analysis. He has taught me how to ask the right questions and work toward the answers. I leave this university secure in the fact that his encyclopedic knowledge of ICP-MS is there for me to consult.

I am also very thankful for the assistance of Lloyd Allen and Dr. Ho-Ming Pang with these projects; I surely would not have completed them as quickly without their help. Lloyd's determination and Ho-Ming's programming expertise will not be forgotten.

Another big thank you should go to the Ames Laboratory machine shop, and especially to Jerry Hand and Steve Lee, both of whom taught me how to approach the construction of my instrument as well as how to do some of my own machining. The splitter itself was constructed by Tim Wolf, whose close work with me and impeccable machining skills allowed the splitter to be constructed to the very best tolerances possible in the machine shop.

I would like to thank my loving parents, Arnold and Vera, who always thought I had potential; I am sure they

are pleased that after all this time I found it and used it to start a career in analytical chemistry.

Finally, I would like to thank Karin Drexler, the love of my life, for giving me a strong reason to complete this work and begin work at a "real" job. She has made me a very happy man.